

Supplementary Information for

Overexpression limits of fission yeast cell-cycle regulators *in vivo* and *in silico*.

Hisao Moriya, Ayako Chino, Orsolya Kapuy, Attila Csikász-Nagy, and Béla Novák

Table of contents

Supplementary Materials and Methods	3
1. Plasmid vectors used in this study.....	3
Table S1. Plasmid used in this study	3
2. Construction of the plasmids	3
Table S2. Oligo DNA primers used for the construction of plasmid vectors.	4
3. Construction of plasmid vectors.....	5
3-1. Construction of pTOWsp series vectors.....	5
Figure S1. Structure of the pTOW vectors.....	5
3-2. Construction of pA6R.....	6
Figure S2. Structure of pA6R.....	6
4. Construction of plasmids with <i>S. pombe cdc</i> genes.....	7
Figure S3. Design of the primers to amplify and clone the target genes.	7
Figure S4. Design of the primers to construct frame-shift mutant genes.....	8
Table S3. Oligo DNA primers to amplify and clone <i>cdc</i> genes in <i>S. pombe</i>	8
5. References for Supplementary Materials and Methods	9
Supplementary Data.....	10
Table S4. Copy numbers of <i>S. pombe</i> gTOW vectors.	10
Table S5. Comparison of the vectors used in gTOW experiment in yeasts.....	10
Figure S5. Examples of gTOW experiments with <i>cdc</i> genes in <i>S. pombe</i> (enlarged part of Figure 2).....	11
Figure S6. Frameshift mutants of <i>rum1</i> and <i>wee1</i> are leaky.....	12
Table S6. Plasmid copy number determined in gTOW experiment.	13
Table S7. Mean GFP fluorescence in gTOW experiment.....	14
Table S8. Comparison of the copy number limits of orthologs in <i>S. pombe</i> and <i>S. cerevisiae</i>	15
Figure S7. Increased copy numbers of cyclin genes do not give <i>cdc</i> phenotype.	16
Table S9. Copy number limits of cell-cycle regulators in the wild type (WT) and cell cycle mutant strains.	17
Supplementary model description and simulation results.....	20
6. Mathematical models of fission yeast cell cycle	20
6.1 A model for DNA replication regulation (“basic model”)	20
6.2 Models to investigate gTOW experiments.....	20
7. Description of the regulatory interactions of cell cycle control network.....	22
Figure S8. Regulatory interactions among cell cycle regulators in the fission yeast cell cycle control network.	22
7.1. Methods to construct a mathematical model of fission yeast cell cycle	24
7.2 Equations and parameters of the models	24
8. The “basic model” (core model).....	25
Figure S9. Different forms of DNA replication origins in the model.	25
Figure S10. Simulation of Hermand & Nurse experiments with the core model.	27

9. The “gTOW model”	28
9.1. Simulation of gTOW experiments.....	29
Figure S11. Three different outcomes in gTOW experiments.....	30
Figure S12. Rum1 overexpression can block mitotic cycle in different way.....	31
Table S10. Investigated mutant phenotypes.....	32
Table S11. Testing gTOW in single deletion mutants <i>in silico</i>	35
10. The “Cdc2-level model”	37
Figure S13. Modeling Cdc2 binding to various cyclins.....	37
Table S12. Testing cyclin competition for Cdc2 <i>in silico</i>	40
11. References for Supplementary model description and simulation results.....	42

Additional files not included in this file

1. **Plasmid_sequences.zip** : This compressed zipped archive contains plasmid sequence files described below.
 - pTOWsp-L.txt : Nucleotide sequence of pTOWsp-L in the GenBank format. The extension .txt should be changed into .dna to open using ApE software.
 - pTOWsp-M.txt : Nucleotide sequence of pTOWsp-M in the GenBank format. The extension .txt should be changed into .dna to open using ApE software.
 - pTOWsp-H.txt : Nucleotide sequence of pTOWsp-H in the GenBank format. The extension .txt should be changed into .dna to open using ApE software.
 - pA6R.txt : Nucleotide sequence of pA6R in the GenBank format. The extension .txt should be changed into .dna to open using ApE software.
2. **ODE_models.zip** : This compressed zipped archive contains ode model files described below.
 - DNArep1_model.txt : This is an ode model file. The extension .txt should be changed into .ode to simulate using XPP-AUT.
 - gTOW_model.txt : This is an ode model file. The extension .txt should be changed into .ode to simulate using XPP-AUT.
 - Cdc2_model.txt : This is an ode model file. The extension .txt should be changed into .ode to simulate using XPP-AUT.
3. **Sp-gTOWmodel_CD.xml** : CellDesigner4.2 file of the gTOW model.
4. **Sp-gTOWmodel.xml**: SBML file of the gTOW model.
5. **Movie S1** : Time-lapse microscopic observation of gTOW experiment with *mik1* + gene.

Supplementary Materials and Methods

1. Plasmid vectors used in this study

Plasmid vectors used in this study are listed in Table S1.

Table S1. Plasmid used in this study.

Plasmid name	Original name	Relevant feature	Source
pRS315		<i>LEU2</i>	Sikorski et al, 1989
pDBlet		<i>ars3002x2, ura4+</i>	Brun et al, 1995
pKT128		<i>EGFP, his5MX</i>	Sheff and Thorn, 2004
mRFP in pRSET-B		<i>mRFP</i>	Campbell et al, 2002
pHM001		pDBlet with <i>LEU2</i>	This study
pHM002		pDBlet with <i>leu2d</i>	This study
pTOWsp-H	pHM004	pHM002 with <i>ura4-EGFP, his5MX</i>	This study
pTOWsp-M	pHM004-835	pHM004 with longer <i>LEU2</i> promoter	This study
pTOWsp-L	pHM004-836	pHM004 with longer <i>LEU2</i> promoter	This study
pHM004-837		pHM004 with longer <i>LEU2</i> promoter	This study
pHM004-838		pHM004 with longer <i>LEU2</i> promoter	This study
pHM004-839		pHM004 with longer <i>LEU2</i> promoter	This study
pHM004-840		pHM004 with longer <i>LEU2</i> promoter	This study
pA6R		pDblet with <i>ade6-mRFP</i> instead of <i>ura4+</i>	This study

2. Construction of the plasmids

For the construction of plasmids, DNA fragments amplified from genome or plasmid were joined using gap-repair method (Oldenburg et al, 1997) in a budding yeast strain BY4741 (*MATa, his3Δ1, leu2Δ0, met15Δ0, ura3Δ0*)(Brachmann et al, 1998). The plasmids constructed in the budding yeast were recovered into *E. coli* (XL1-blue, Agilent Technologies), and the structures were checked with restriction enzyme digestions and partial nucleotide sequencings. All DNA fragments were amplified with polymerase chain reaction (PCR) using the high fidelity DNA polymerase KODplus (Toyobo) as described in the manufacturer's protocol. Oligo DNA primers used for the construction of plasmid vectors are shown in Table S2.

Table S2. Oligo DNA primers used for the construction of plasmid vectors.

Oligo	Sequence (5' to 3')
OSBI0009	GGAAACAGCTATGACCATG
OSBI0582	gcatctgtcggtatccacaccgCATATGaatggtcaggtcattgagtg
OSBI0583	agattgtactgagagtgcac
OSBI0584	GGGATTGTAGCTAACGCTCCATATGcctaacaataacgagaacacacagg
OSBI0585	cctgtgttttcgttatgttggaggCATATGGAGCTTAGCTACAAATCCC
OSBI0606	GGGATTGTAGCTAACGCTCCATATGtataatatattcaaggatataccat
OSBI0607	atggtataatccttcaaataatataCATATGGAGCTTAGCTACAAATCCC
OSBI0640	gcgcgttcggtgatgacgg
OSBI0719	tgttaattaaaccacgcaccgtcaccATGCTGAGAAAGTCTTGCTGATATG
OSBI0720	CATATCAGCAAAGACTTCAGCATggtgacgggtcggttaattaaca
OSBI0721	CTTAACATATGCCAGTGGGATTGTAGCTAACGCTCCATATGttcttacctttacattca
OSBI0835	TACATATAGCCAGTGGGATTGTAGCTAACGCTCCATATGttcttacctttacattca
OSBI0836	TACATATAGCCAGTGGGATTGTAGCTAACGCTCCATATGgtggtagcaatcgcttac
OSBI0837	TACATATAGCCAGTGGGATTGTAGCTAACGCTCCATATGtatttaaggacctattgttt
OSBI0838	TACATATAGCCAGTGGGATTGTAGCTAACGCTCCATATGttgcatcacaataacttgaag
OSBI0839	TACATATAGCCAGTGGGATTGTAGCTAACGCTCCATATGtagaatagagaagcggtcat
OSBI0840	TACATATAGCCAGTGGGATTGTAGCTAACGCTCCATATGaggtgagagcgccggAACCG
OSBI0850	TTACCAATGCTTAATCAGTG
OSBI0851	ATGAGTATTCAACATTCCG
OSBI0880	attaccctgttatccctagcggtccaaatcaactacatctttaataat
OSBI0881	attattaaaagatgttagttgatggatccgctaggataacaggtaat
OSBI0882	ccatgttcaatgtcggtatcactacaatgacctgaccattCATATGcg
OSBI0883	ccgCATATGaatggtcaggtcattgttagtgatacgcacattgaaacatgg
OSBI0884	aaaagcaagcaaaatcattaacagTTAGGCGCCGGTGGAGTGGCGGCC
OSBI0885	GGGCCGCCACTCCACCAGGCGCCTAActgttaatgatttgcttgcttt
OSBI0886	TGATGACGTCCCTCGGAGGAGGCCATTGAGAATAATTTCCAACCAAC
OSBI0887	GTTGGTTGGAAAAATTATTCTGCAATGGCCTCCTCGAGGACGTCATCA

3. Construction of plasmid vectors

3-1. Construction of pTOWsp series vectors.

The construction of pTOWsp series vectors is described below. The structures of the vectors are shown in Figure S1.

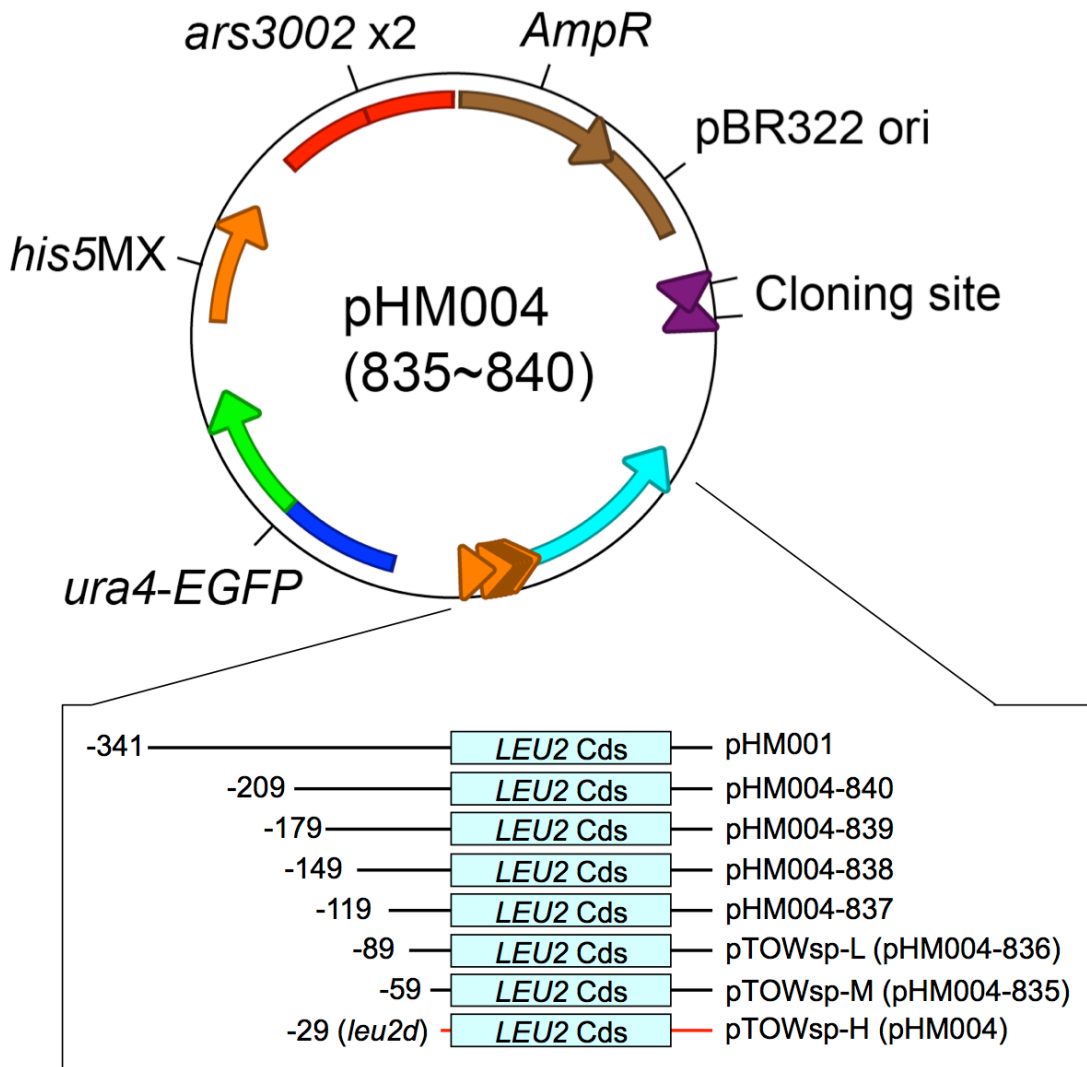


Figure S1. Structure of the pTOW vectors.

Step1: Construction of pHM001

1. Amplify budding yeast *LEU2* gene using pRS315 as a template with primers OSBI0582-0584.
2. Amplify fission yeast *ura4+* gene using pDBlet as a template with primers OSBI0583-0585.
3. Cut pDBlet with a restriction enzyme *NdeI*.
4. Join the 1~3 DNA fragments with Gap-Repair method.

Step2: Construction of pHM002

1. Amplify budding yeast *leu2d* gene using pRS315 as a template, with primers OSBI0582-0606.
2. Amplify fission yeast *ura4+* using pDBlet as a template, with primers OSBI0583-0607.
3. Cut pDBlet with a restriction enzyme *NdeI*.

- Join 1~3 DNA fragments with Gap-Repair method.

Step3: Construction of pHM004

- Amplify a DNA fragment containing *leu2d* and *ura4+* genes using pHM002 as a template, with primers OSBI009-0719.
- Amplify *EGFP-sphis5MX* cassette using pKT128 as a template, with primers OSBI0720-0721.
- Cut pDBlet with a restriction enzyme *NdeI*.
- Join 1~3 DNA fragments with Gap-Repair method.

Step4: Construction of pHM004-835~840

- Amplify DNA fragments containing *LEU2* genes with deletions of the promoter using pHM001 as a template, with primers OSBI009-0835~840.
- Amplify *ura4-EGFP-sphis5MX* gene cassette using pHM004 as a template, with primers OSBI0585-0640.
- Cut pDBlet with a restriction enzyme *NdeI*.
- Join 1~3 DNA fragments with Gap-Repair method.

Step5: Changing vector's names

We have measured the copy number of the pHM004-835-840 in -leucine condition (Table S4). And select three plasmids for further use. We thus changed the names of the vectors as follows.

- pHM004 (*LEU2* promoter length is 29bp) : pTOWsp-H
- pHM004-835 (*LEU2* promoter length is 59bp) : pTOWsp-M
- pHM004-836 (*LEU2* promoter length is 89bp) : pTOWsp-L

3-2. Construction of pA6R

The construction of pA6R vector is described below. The structure of the plasmid is shown in Figure S2.

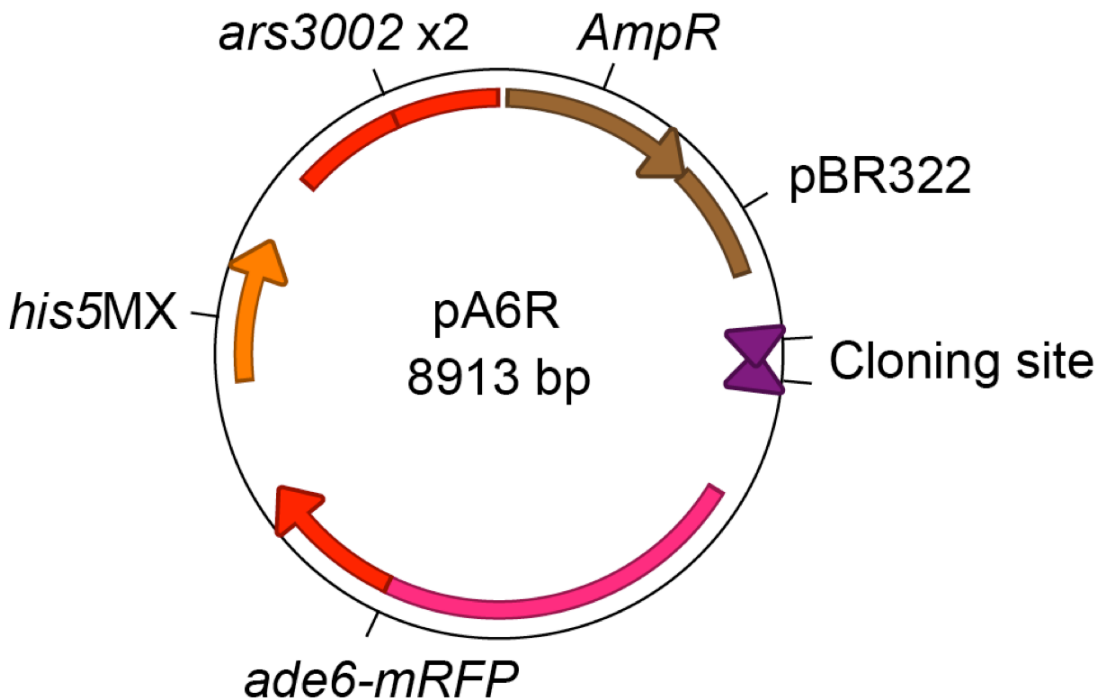


Figure S2. Structure of pA6R.

- Amplify two DNA fragments containing the plasmid backbone using pHM004 as a

- template with primers OSBI0881-0850 and OSBI0851-0882, respectively
2. Amplify two DNA fragments containing *ade6* (promoter and ORF) and *ade6* terminator using *S. pombe* genome as a template with primers OSBI0883-0886 and OSBI0880-0885, respectively.
 3. Amplify a DNA fragment containing *mRFP* using *mRFP* in pRSET-B as a template with primers OSBI0884-0887.
 4. Join 5 DNA fragments above with the Gap-Repair method.

4. Construction of plasmids with *S. pombe cdc* genes

Each target gene studied in this work was cloned from just after its upstream ORFs to just before its downstream ORFs, so that it contains all of its regulatory elements (i.e. its native promoter and terminator). Figure S3 is the case of *cdc2*, as an example. According to the genome annotations and nucleotide sequences obtained from *Schizosaccharomyces pombe* GeneDB (<http://old.genedb.org/genedb/pombe/>), we used 23bp in the end of neighboring ORFs for the priming sites to amplify each target gene with PCR (Figure S3 as an example). Each primer contains homologous sequence with vectors at its 5' for the gap-repair cloning. Each upstream (Up) primer and downstream (Down) primer contains *HindIII* site (aagctt) and *KpnI* site (ggtacc), respectively, for the verification of construction. Oligo DNA primers to amplify and clone the target genes are listed in Table S3.

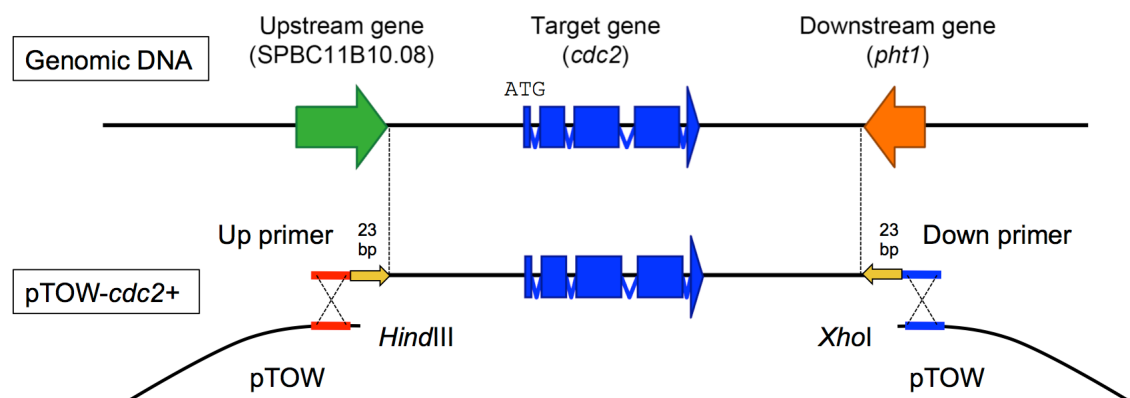


Figure S3. Design of the primers to amplify and clone the target genes.

Each target gene was amplified with the primer set from FY7652 genome with high fidelity PCR. The amplified DNA fragment was joined with the vectors digested with *HindIII* and *XhoI* in advance using gap-repair method in *S. cerevisiae*. *his5MX* was used as the selection marker of plasmid in *S. cerevisiae*. At least two independent plasmids for each construction were recovered from yeast into *E. coli*, and purified for structural verifications with restriction enzyme digestion and sequencing. *cut1* was amplified as two fragments and joined them into vectors with gap-repair method, because it was too large to amplify by single PCR (eF primer and eR primer were used for the purpose).

For the construction of frameshift mutant of each gene, two DNA fragments were amplified with the primers with cgca insertion just after start codon, and joined them into the vectors with gap-repair method. Each frameshift mutant gene thus contains *FspI* site (tgcgca) in the beginning of ORF. Figure S4 is the case of *cdc2*, as an example.

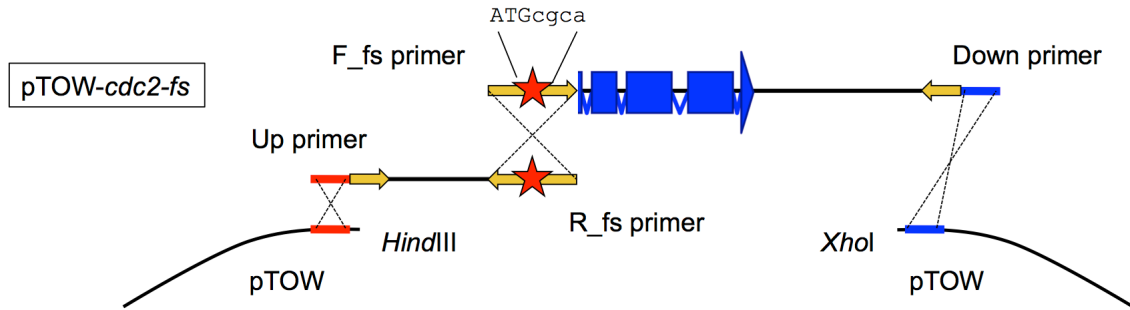


Figure S4. Design of the primers to construct frame-shift mutant genes.

Table S3. Oligo DNA primers to amplify and clone *cdc* genes in *S. pombe*.

No.	Gene	Up primer	Sequence (5' to 3')	Down primer	Sequence (5' to 3')
1	<i>ark1+</i>	OSBI0667	agctatgaccatgattacgccaagcttGGGGTTCGATTCCCCCTGACGGA	OSBI0668	gactcaactataggcgaaattgggtaccTCATTCTTCGTCTAGTCTATTG
2	<i>cdc2+</i>	OSBI0608	agctatgaccatgattacgccaagcttGACTTGGCAATGATTCTTTTA	OSBI0609	gactcaactataggcgaaattgggtaccCCCGAGGAGAAATTATTATTA
3	<i>cdc7+</i>	OSBI0669	agctatgaccatgattacgccaagcttCATAACCATCAGACACTTGTGTTA	OSBI0670	gactcaactataggcgaaattgggtaccTATATTCTTTTACTTCTGACA
4	<i>cdc10+</i>	OSBI0671	agctatgaccatgattacgccaagcttAGTGAAAACGTTGTGTTAAGTAA	OSBI0672	gactcaactataggcgaaattgggtaccGAAAATTAACTAATTCCAATA
5	<i>cdc13+</i>	OSBI0610	agctatgaccatgattacgccaagcttAGGCCCTTGTCTCTTCCCTATGA	OSBI0611	gactcaactataggcgaaattgggtaccGTAATCGATCTACTATTGATTA
6	<i>cdc16+</i>	OSBI0673	agctatgaccatgattacgccaagcttAGCGCTGAATTGGGAGTCGACA	OSBI0674	gactcaactataggcgaaattgggtaccTCCTTGCTATGCATACGACCCA
7	<i>cdc18+</i>	OSBI0675	agctatgaccatgattacgccaagcttAAAGATGTAGAAAAAGAAGATA	OSBI0676	gactcaactataggcgaaattgggtaccCGTGTGTTTTGTGGACTCTTTA
8	<i>cdc25+</i>	OSBI0612	agctatgaccatgattacgccaagcttCTGCCGAGCATTTAAGAATT	OSBI0613	gactcaactataggcgaaattgggtaccCTTGGAAAGCATGGTCGTTATTCA
9	<i>chk1+</i>	OSBI0677	agctatgaccatgattacgccaagcttCTGGTTTGATATCAGAATCAA	OSBI0678	gactcaactataggcgaaattgggtaccATATTGGGTAAATGATGTATTA
10	<i>cig1+</i>	OSBI0679	agctatgaccatgattacgccaagcttATCTGATTCAAATTCGAATCTCA	OSBI0680	gactcaactataggcgaaattgggtaccAATTCCCTGATATTAAATCAACA
11	<i>cig2+</i>	OSBI0681	agctatgaccatgattacgccaagcttAGCGCTATTGCTGAATACTGTGTT	OSBI0682	gactcaactataggcgaaattgggtaccAAAAAAAGCTAAATGTTCAATTA
12	<i>clp1+</i>	OSBI0683	agctatgaccatgattacgccaagcttCTGCTCTTGAAGTTAATGTTG	OSBI0684	gactcaactataggcgaaattgggtaccAAACTGACCCAAAGGTGAAACAA
13	<i>csk1+</i>	OSBI0685	agctatgaccatgattacgccaagcttCAGCTTTAAATTAACTCGCA	OSBI0686	gactcaactataggcgaaattgggtaccAAACTCCACGACTTCCAAATCCA
14	<i>cut1+</i>	OSBI0687	agctatgaccatgattacgccaagcttTGCGGCCATTAGTGGCAGACA	OSBI0742	gctaatttcgcattattgtggattatgccttaggagattttggtcacc
15	<i>cut2+</i>	OSBI0689	agctatgaccatgattacgccaagcttACATGCGACGTTGTGTCGCCCC	OSBI0690	gactcaactataggcgaaattgggtaccTACATCAAGGCTGCTAAGTTTA
16	<i>dfp1+</i>	OSBI0691	agctatgaccatgattacgccaagcttTGACACGAAAGGAGAAATATA	OSBI0692	gactcaactataggcgaaattgggtaccCTTCTGAAATCATATGAGTC
17	<i>fkh2+</i>	OSBI0693	agctatgaccatgattacgccaagcttACGAGATACATCGCCGGAGACA	OSBI0694	gactcaactataggcgaaattgggtaccGGGAGATCGTGAATGCGCAGAC
18	<i>hsk1+</i>	OSBI0695	agctatgaccatgattacgccaagcttCTAGAAAAGATCCAACGACA	OSBI0696	gactcaactataggcgaaattgggtaccGGTGTGTTGAGCTCATTGCTA
19	<i>mik1+</i>	OSBI0697	agctatgaccatgattacgccaagcttTGTTGCAAAATTCTTTTTTTT	OSBI0698	gactcaactataggcgaaattgggtaccTCGTGAATTATTAAAAGAT
20	<i>plo1+</i>	OSBI0699	agctatgaccatgattacgccaagcttATTATGCACATTTATCCATA	OSBI0700	gactcaactataggcgaaattgggtaccGATATGCGTTCTGGGATACCTCA
21	<i>puc1+</i>	OSBI0701	agctatgaccatgattacgccaagcttTATGAGCACAAATTGGCTCGTA	OSBI0702	gactcaactataggcgaaattgggtaccAGAAAATTAAAAAAACTCACTA
22	<i>ras1+</i>	OSBI0703	agctatgaccatgattacgccaagcttATCTTGAGAAAATCACATCCCTA	OSBI0704	gactcaactataggcgaaattgggtaccAAAGCCTTTAGGGATAGATTG
23	<i>res1+</i>	OSBI0705	agctatgaccatgattacgccaagcttAGCAGCAGTACCAAGCAAATG	OSBI0706	gactcaactataggcgaaattgggtaccGCAGGAATTGACGTCGAATTGTA
24	<i>res2+</i>	OSBI0707	agctatgaccatgattacgccaagcttACGTTACTGGGAAATGCTCATA	OSBI0708	gactcaactataggcgaaattgggtaccTGTCAAAACTTTCAACGCATCCA
25	<i>rum1+</i>	OSBI0614	agctatgaccatgattacgccaagcttTTCTTGTTGCAATTAGCTGATCA	OSBI0615	gactcaactataggcgaaattgggtaccTTCTGGGATTGTTGATCA
26	<i>sid2+</i>	OSBI0709	agctatgaccatgattacgccaagcttAAAAATGGCAAGTTAATAGCTG	OSBI0710	gactcaactataggcgaaattgggtaccTTAACAGATAATTACAGGTGA
27	<i>s/p1+</i>	OSBI0711	agctatgaccatgattacgccaagcttAAAAGAACGTAATAGGAACATCA	OSBI0712	gactcaactataggcgaaattgggtaccACTACCCGTTCTATTCCGTTCA
28	<i>spg1+</i>	OSBI0713	agctatgaccatgattacgccaagcttATCAAAACTACAATTAAACTTG	OSBI0714	gactcaactataggcgaaattgggtaccACAGTTGAACGTTAGAAATATA
29	<i>srw1+</i>	OSBI0715	agctatgaccatgattacgccaagcttTACGCGAACATTAGCTGTAGACA	OSBI0716	gactcaactataggcgaaattgggtaccACAAATGCAAAGCCTCTCAATT
30	<i>wee1+</i>	OSBI0616	agctatgaccatgattacgccaagcttGACAGAACAGTTTGGCTCA	OSBI0617	gactcaactataggcgaaattgggtaccAGAAAATTACGTCCTCCAAGCA
31	<i>pyp3+</i>	OSBI0717	agctatgaccatgattacgccaagcttGTAAAAGGGTGGATGGATATATA	OSBI0718	gactcaactataggcgaaattgggtaccATGTAATAGGATGGGAGCATCA
32	<i>byr4+</i>	OSBI	agctatgaccatgattacgccaagcttGGCTAACGTTAATGTCAGACAT	OSBI	gactcaactataggcgaaattgggtaccACCTCCTGGCAACCCCAATAA
		F_fs primer		R_fs primer	
2_fs	<i>cdc2-fs</i>	OSBI0725	tcttttaggtttgcaATGcgcaGAGAATTATCATAAAAGTCGA	OSBI0726	TCGACTTTTGATAATTCTCtgcgCATgcacaccactaaaaga
5_fs	<i>cdc13-fs</i>	OSBI0727	cgtttctttttccATGcgcaACTACCGCTGTTAACCTCG	OSBI0728	CGAGTTAAACGACGGTAGTTcgCATgaggaaaagaagaaac
8_fs	<i>cdc25-fs</i>	OSBI0729	gttaaacctcaactaaaATGcgcaGATTCTCCGCTTCTTCACT	OSBI0730	AGTGAAGAAAGCGGAGATCtgcgCATtttaggtggat
25_fs	<i>rum1-fs</i>	OSBI0731	tggattgtcagtgcgtATGcgcaGAACCTCAACACACCTAT	OSBI0732	ATAGGTGGTGTGAAGGTTctcgcatAgcgaactgacaatcc
30_fs	<i>wee1-fs</i>	OSBI0733	acattttccatagaaaaATGcgcaAGCTCTCTCTAATAC	OSBI0734	GTATTAGAAGAAGAGCTtgcgCATtttaggtatggaaaatgt
		eF primer		eR primer	
14	<i>cut1+</i>	OSBI0768	ggtgaccaaaaatctcttagagataatccaaacaataatgcgaaattgc	OSBI0769	gctaatttcgcattattgtggattatgccttaggagattttggtcacc

5. References for Supplementary Materials and Methods

Brachmann CB, Davies A, Cost GJ, Caputo E, Li J, Hieter P, Boeke JD (1998) Designer deletion strains derived from *Saccharomyces cerevisiae* S288C: a useful set of strains and plasmids for PCR-mediated gene disruption and other applications. *Yeast* **14**: 115-132

Brun C, Dubey DD, Huberman JA (1995) pDblet, a stable autonomously replicating shuttle vector for *Schizosaccharomyces pombe*. *Gene* **164**: 173-177

Campbell RE, Tour O, Palmer AE, Steinbach PA, Baird GS, Zacharias DA, Tsien RY (2002) A monomeric red fluorescent protein. *Proc Natl Acad Sci U S A* **99**: 7877-7882

Oldenburg KR, Vo KT, Michaelis S, Paddon C (1997) Recombination-mediated PCR-directed plasmid construction in vivo in yeast. *Nucleic Acids Res* **25**: 451-452

Sheff MA, Thorn KS (2004) Optimized cassettes for fluorescent protein tagging in *Saccharomyces cerevisiae*. *Yeast* **21**: 661-670

Sikorski RS, Hieter P (1989) A system of shuttle vectors and yeast host strains designed for efficient manipulation of DNA in *Saccharomyces cerevisiae*. *Genetics* **122**: 19-27

Supplementary Data

Table S4. Copy numbers of *S. pombe* gTOW vectors.

Plasmid name	<i>LEU2</i> promoter ^{*1}	Copy number ± SD ^{*2}
pHM001	-341 (LEU2)	5.9 ± 2.1
pHM004-840	-209	63.1 ± 1.2
pHM004-839	-179	80.9 ± 15.6
pHM004-838	-149	89.2 ± 9.2
pHM004-837	-119	78.8 ± 8.1
pTOWsp-L	-89	41.3 ± 13.0
pTOWsp-M	-59	55.4 ± 11.3
pTOWsp-H	-29 (leu2d)	116.8 ± 7.0

*1 Length from ATG is shown with negative number.

*2 Copy number in leucine- condition.

Table S5. Comparison of the vectors used in gTOW experiment in yeasts.

Species	Vector Name	Plasmid Origin	1st selection	2nd selection	Others
<i>S. cerevisiae</i>	pTOW (pSBI40)	2μ DNA	<i>URA3</i>	<i>leu2d</i>	
<i>S. pombe</i>	pTOWsp-H, -M, -L	<i>ars3002</i> x2	<i>ura4+</i>	<i>LEU2</i> derivative	<i>EGFP-sphis5MX</i>

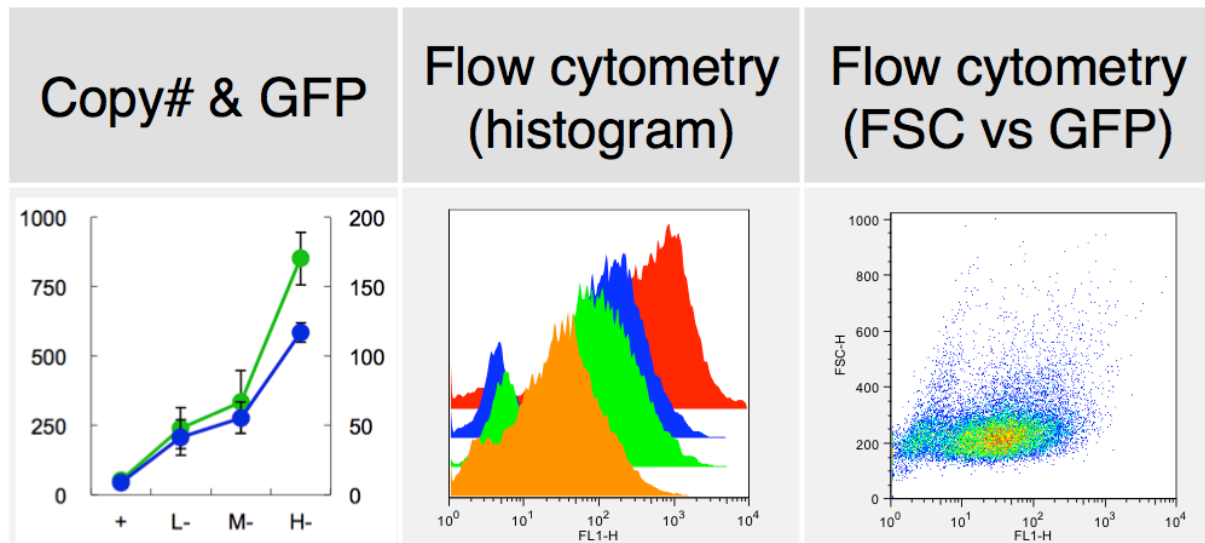


Figure S5. Examples of gTOW experiments with *cdc* genes in *S. pombe* (enlarged part of Figure 2).

The experimental results obtained by gTOW with empty vector.

1st column: The plasmid copy number (blue graph, right vertical axis) and the mean GFP fluorescence (green graph, left vertical axis) in gTOW in leucine+ (indicated as "+") and leucine- with each vector (pTOWsp-L, -M and -H) are shown (indicated as "L-", "M-", and "H-", respectively).

2nd column: Cell distribution (histogram) with GFP fluorescence in gTOW experiments in leucine+ (orange graph) and leucine- conditions with -L vector (green graph), -M vector (blue graph), and -H vector (red graph) are shown.

3rd column: Scatter plot between GFP fluorescence (FL-1) and cell size (FSC). Cells were cultured in the leucine+ condition.

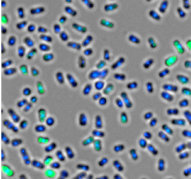
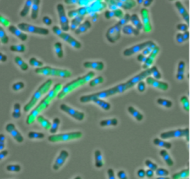
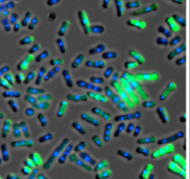
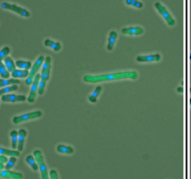
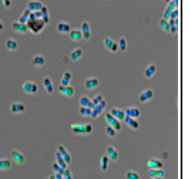
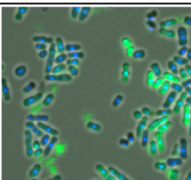
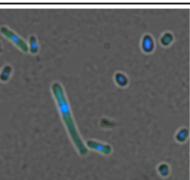
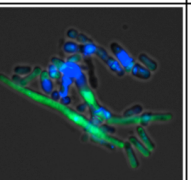
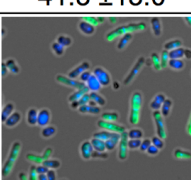
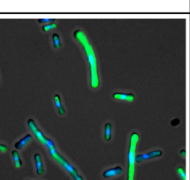
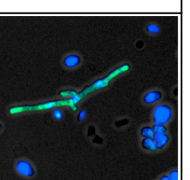
	vector	<i>rum1+</i>	<i>rum1-fs</i>	<i>wee1+</i>	<i>wee1-fs</i>
leucine+					
	8.5 ±3.3	2.4 ±0.4	2.1 ±0.2	0.9 ±0.4	6.2 ±1.0
L vector leucine-					
	41.3 ±13.0	12.9 ±2.2		2.4 ±0.8	
H vector leucine-					
	116.8 ±7.0		89.8 ±11.5		58.8 ±24.3

Figure S6. Frameshift mutants of *rum1* and *wee1* are leaky.

Each cell has pTOW plasmid with indicated gene, cultured in indicated condition. GFP fluorescence, nucleus and septum were observed. Plasmid copy number is indicated under the picture.

Table S6. Plasmid copy number determined in gTOW experiment.

No.	Gene Name	Plasmid copy number (\pm SD)*1			
		+leucine	L (-leucine)	M (-leucine)	H (-leucine)
	vector	8.5 \pm 3.3	41.3 \pm 13.0	55.4 \pm 11.3	116.8 \pm 7.0
1	<i>ark1+</i>	7.2 \pm 4.5	36.1 \pm 7.2	63.0 \pm 11.4	149.0 \pm 18.2
2	<i>cdc2+</i>	2.4 \pm 1.1	26.2 \pm 4.4	52.1 \pm 8.8	97.0 \pm 12.1
3	<i>cdc7+</i>	2.0 \pm 0.8	8.7 \pm 0.7	10.5 \pm 1.9	2.5 \pm 1.0
4	<i>cdc10+</i>	8.2 \pm 1.2	27.7 \pm 5.1	66.1 \pm 7.9	69.5 \pm 10.6
5	<i>cdc13+</i>	1.4 \pm 0.7	4.5 \pm 1.9	2.3 \pm 0.9	1.5 \pm 0.7
6	<i>cdc16+</i>	5.7 \pm 2.6	31.2 \pm 3.0	48.2 \pm 3.5	106.0 \pm 12.2
7	<i>cdc18+</i>	6.0 \pm 3.6	28.7 \pm 6.6	39.0 \pm 4.8	44.2 \pm 7.8
8	<i>cdc25+</i>	3.8 \pm 2.0	22.6 \pm 3.4	38.7 \pm 15.1	29.4 \pm 13.7
9	<i>chk1+</i>	5.4 \pm 1.3	35.2 \pm 9.3	55.9 \pm 4.6	112.7 \pm 18.0
10	<i>cig1+</i>	3.7 \pm 1.6	17.5 \pm 4.9	42.8 \pm 20.1	1.9 \pm 0.6
11	<i>cig2+</i>	1.6 \pm 0.7	15.9 \pm 6.8	14.9 \pm 4.7	1.4 \pm 0.7
12	<i>clp1+</i>	1.6 \pm 1.0	6.9 \pm 3.2	5.0 \pm 0.3	2.3 \pm 2.6
13	<i>csk1+</i>	9.5 \pm 3.2	52.9 \pm 19.9	77.7 \pm 9.6	218.0 \pm 7.4
14	<i>cut1+</i>	2.9 \pm 0.7	43.5 \pm 8.1	56.6 \pm 21.3	3.0 \pm 0.7
15	<i>cut2+</i>	5.8 \pm 2.2	26.0 \pm 3.8	32.2 \pm 4.6	10.3 \pm 13.5
16	<i>dfp1+</i>	5.2 \pm 2.4	26.8 \pm 4.5	41.3 \pm 4.0	70.3 \pm 5.4
17	<i>fkh2+</i>	5.6 \pm 1.2	17.6 \pm 2.0	24.5 \pm 2.2	4.9 \pm 1.0
18	<i>hsk1+</i>	8.8 \pm 4.7	43.5 \pm 8.7	77.7 \pm 13.2	200.2 \pm 12.4
19	<i>mik1+</i>	5.3 \pm 3.7	39.5 \pm 8.2	65.9 \pm 6.6	102.8 \pm 7.5
20	<i>plo1+</i>	6.3 \pm 2.1	34.7 \pm 7.7	31.9 \pm 3.6	3.8 \pm 2.2
21	<i>puc1+</i>	5.2 \pm 2.0	30.3 \pm 3.6	72.9 \pm 8.6	154.9 \pm 30.5
22	<i>ras1+</i>	8.8 \pm 1.5	38.4 \pm 2.6	77.8 \pm 8.5	105.1 \pm 29.1
23	<i>res1+</i>	3.8 \pm 1.9	24.6 \pm 1.1	28.3 \pm 7.4	17.1 \pm 9.2
24	<i>res2+</i>	4.2 \pm 1.7	31.6 \pm 2.4	75.9 \pm 9.2	161.6 \pm 35.2
25	<i>rum1+</i>	2.4 \pm 0.4	12.9 \pm 2.2	13.8 \pm 2.3	3.8 \pm 1.7
26	<i>sid2+</i>	6.8 \pm 4.0	31.6 \pm 3.8	62.5 \pm 8.2	143.0 \pm 11.5
27	<i>slp1+</i>	4.0 \pm 1.5	27.7 \pm 1.6	26.2 \pm 10.3	2.8 \pm 2.4
28	<i>spg1+</i>	0.6 \pm 0.5	0.9 \pm 0.5	0.9 \pm 0.3	1.0 \pm 0.3
29	<i>srw1+</i>	5.4 \pm 2.1	32.5 \pm 7.7	57.5 \pm 9.1	114.7 \pm 19.1
30	<i>wee1+</i>	0.9 \pm 0.4	2.4 \pm 0.8	2.0 \pm 1.0	2.3 \pm 1.3
31	<i>pyp3+</i>	11.1 \pm 3.1	39.9 \pm 8.7	60.5 \pm 7.2	187.0 \pm 24.5
2_fs	<i>cdc2-fs</i>	13.1 \pm 1.5			181.4 \pm 4.7
5_fs	<i>cdc13-fs</i>	11.0 \pm 0.4			173.3 \pm 30.6
8_fs	<i>cdc25-fs</i>	10.4 \pm 2.6			231.1 \pm 42.9
25_fs	<i>rum1-fs</i>	2.1 \pm 0.2			89.8 \pm 11.5
30_fs	<i>wee1-fs</i>	6.2 \pm 1.0			58.8 \pm 24.3

*1 L, M, and H stand the experiments done with pTOWsp-L, pTOWsp-M, and pTOWsp-H, respectively. Numbers in bold letters were used as copy number limits.

Table S7. Mean GFP fluorescence in gTOW experiment.

No.	Gene Name	Mean GFP fluorescence (\pm SD)*1			
		+leucine	L (-leucine)	M (-leucine)	H (-leucine)
	vector	52.5 \pm 8.4	239.9 \pm 73.5	334.6 \pm 113.4	851.5 \pm 94.9
1	<i>ark1+</i>	48.1 \pm 9.2	202.6 \pm 58.8	349.2 \pm 131.6	709.5\pm 84.4
2	<i>cdc2+</i>	25.6 \pm 3.7	175.0 \pm 29.3	305.0 \pm 33.3	520.3\pm 63.5
3	<i>cdc7+</i>	30.3 \pm 13.6	72.9 \pm 44.1	81.7\pm 66.1	13.6 \pm 3.4
4	<i>cdc10+</i>	42.6 \pm 10.9	172.8 \pm 35.4	319.3 \pm 36.1	379.8\pm 62.7
5	<i>cdc13+</i>	17.4 \pm 1.6	33.0\pm 5.0	27.4 \pm 5.9	10.8 \pm 2.4
6	<i>cdc16+</i>	38.5 \pm 7.2	129.5 \pm 26.1	207.5 \pm 80.5	443.8\pm 69.8
7	<i>cdc18+</i>	44.1 \pm 8.9	163.0 \pm 24.2	221.2 \pm 33.4	179.0\pm 8.3
8	<i>cdc25+</i>	22.7 \pm 2.0	185.0 \pm 16.1	317.8\pm 58.5	85.0 \pm 41.0
9	<i>chk1+</i>	44.9 \pm 7.8	189.4 \pm 46.5	338.0 \pm 53.3	543.0\pm 60.0
10	<i>cig1+</i>	24.3 \pm 5.0	132.8 \pm 23.1	331.0\pm 142.7	18.6 \pm 5.4
11	<i>cig2+</i>	16.2 \pm 1.2	75.2\pm 8.6	96.2 \pm 9.5	13.9 \pm 6.5
12	<i>clp1+</i>	21.0 \pm 3.3	47.4\pm 13.2	47.2 \pm 6.3	12.8 \pm 7.9
13	<i>csk1+</i>	51.5 \pm 7.7	215.6 \pm 91.0	416.5 \pm 155.0	956.0\pm 59.4
14	<i>cut1+</i>	32.7 \pm 15.2	204.8 \pm 87.2	433.2\pm 61.0	23.1 \pm 5.3
15	<i>cut2+</i>	32.5 \pm 4.8	110.3 \pm 17.0	176.8\pm 15.6	58.6 \pm 24.9
16	<i>dfp1+</i>	39.7 \pm 8.2	135.4 \pm 27.3	226.8 \pm 23.6	310.0\pm 32.1
17	<i>fkh2+</i>	29.3 \pm 5.9	141.6 \pm 19.4	165.0\pm 9.5	24.1 \pm 5.8
18	<i>hsk1+</i>	45.0 \pm 8.5	161.8 \pm 74.2	361.8 \pm 87.8	791.0\pm 79.0
19	<i>mik1+</i>	43.2 \pm 8.9	186.6 \pm 57.4	320.0 \pm 82.2	430.3\pm 33.1
20	<i>plo1+</i>	39.5 \pm 8.2	151.0\pm 74.2	146.8 \pm 63.4	30.0 \pm 16.0
21	<i>puc1+</i>	37.4 \pm 10.0	141.7 \pm 8.4	486.0 \pm 170.4	765.5\pm 17.7
22	<i>ras1+</i>	34.9 \pm 5.1	185.3 \pm 69.2	490.6 \pm 58.9	472.5\pm 115.5
23	<i>res1+</i>	34.6 \pm 1.8	164.3 \pm 15.5	259.8\pm 58.0	133.5 \pm 34.0
24	<i>res2+</i>	37.9 \pm 8.6	189.0 \pm 61.5	393.2 \pm 98.4	897.0\pm 110.2
25	<i>rum1+</i>	24.1 \pm 2.7	84.4 \pm 8.4	94.2\pm 4.3	20.5 \pm 2.9
26	<i>sid2+</i>	42.0 \pm 7.4	160.0 \pm 58.3	255.4 \pm 68.3	694.3\pm 91.4
27	<i>slp1+</i>	28.8 \pm 3.3	175.4\pm 11.4	193.0 \pm 17.2	22.9 \pm 3.6
28	<i>spg1+</i>	10.1 \pm 2.4	14.2\pm 1.5	8.8 \pm 2.0	4.7 \pm 0.5
29	<i>srw1+</i>	41.7 \pm 6.1	236.3 \pm 91.5	366.0 \pm 65.1	780.8\pm 85.8
30	<i>wee1+</i>	16.0 \pm 3.5	21.9\pm 0.5	13.7 \pm 11.9	7.1 \pm 2.4
31	<i>pyp3+</i>	41.7 \pm 9.1	224.9 \pm 156.5	247.0 \pm 16.7	722.8\pm 116.6
2_fs	<i>cdc2-fs</i>	44.8 \pm 11.4			827.0\pm 72.8
5_fs	<i>cdc13-fs</i>	40.0 \pm 6.7			724.5\pm 61.1
8_fs	<i>cdc25-fs</i>	37.0 \pm 5.8			731.3\pm 118.8
25_fs	<i>rum1-fs</i>	38.8 \pm 3.9			433.0\pm 63.2
30_fs	<i>wee1-fs</i>	39.8 \pm 4.4			273.5\pm 78.7

*1 L, M, and H stand the experiments done with pTOWsp-L, pTOWsp-M, and pTOWsp-H, respectively. Numbers in bold letters were used as upper limits.

Table S8. Comparison of the copy number limits of orthologs in *S. pombe* and *S. cerevisiae*.

Functional Category	<i>S. pombe</i>		<i>S. cerevisiae</i> *	
	Gene	Copy #	Copy #	Gene
CDK	<i>cdc2+</i>	97.0	83.7	<i>CDC28</i>
G1 cyclin	<i>puc1+</i>	154.9	55.7	<i>CLN1</i>
			115.9	<i>CLN2</i>
			181.2	<i>CLN3</i>
B-type cyclin	<i>cdc13+</i>	4.5	71.1	<i>CLB1</i>
			30.3	<i>CLB2</i>
	<i>cig1+</i>	42.8	17.9	<i>CLB3</i>
			104.8	<i>CLB4</i>
G1 transcription factor	<i>cdc10+</i>	69.5	12.8	<i>CLB5</i>
			154.3	<i>CLB6</i>
			141.2	
MCM loader	<i>cdc18+</i>	44.2	154.3	<i>SWI6</i>
			28.3	<i>SWI4</i>
			161.6	<i>MBP1</i>
CDK inhibitor	<i>rum1+</i>	13.8	30.9	<i>SIC1</i>
CDK-tyrosine kinase	<i>wee1+</i>	2.4	22.8	<i>SWE1</i>
	<i>mik1+</i>	102.8		
CDK-tyrosine phosphatase	<i>cdc25+</i>	38.7	197.0	<i>MIH1</i>
	<i>pyp3+</i>	187.0		
SIN / MEN components	<i>cdc16+</i>	106.0	127.9	<i>BUB2</i>
	<i>cdc7+</i>	10.5	166.6	<i>CDC15</i>
	<i>clp1+</i>	6.9	0.8	<i>CDC14</i>
	<i>spg1+</i>	0.9	86.7	<i>TEM1</i>
Separase	<i>cut1+</i>	56.6	163.7	<i>ESP1</i>
Securin	<i>cut2+</i>	32.2	55.8	<i>PDS1</i>
APC activator	<i>srw1+</i>	114.7	62.1	<i>CDH1</i>
	<i>s/p1+</i>	27.7	69.6	<i>CDC20</i>

* Data in Moriya et al, 2006 was used.

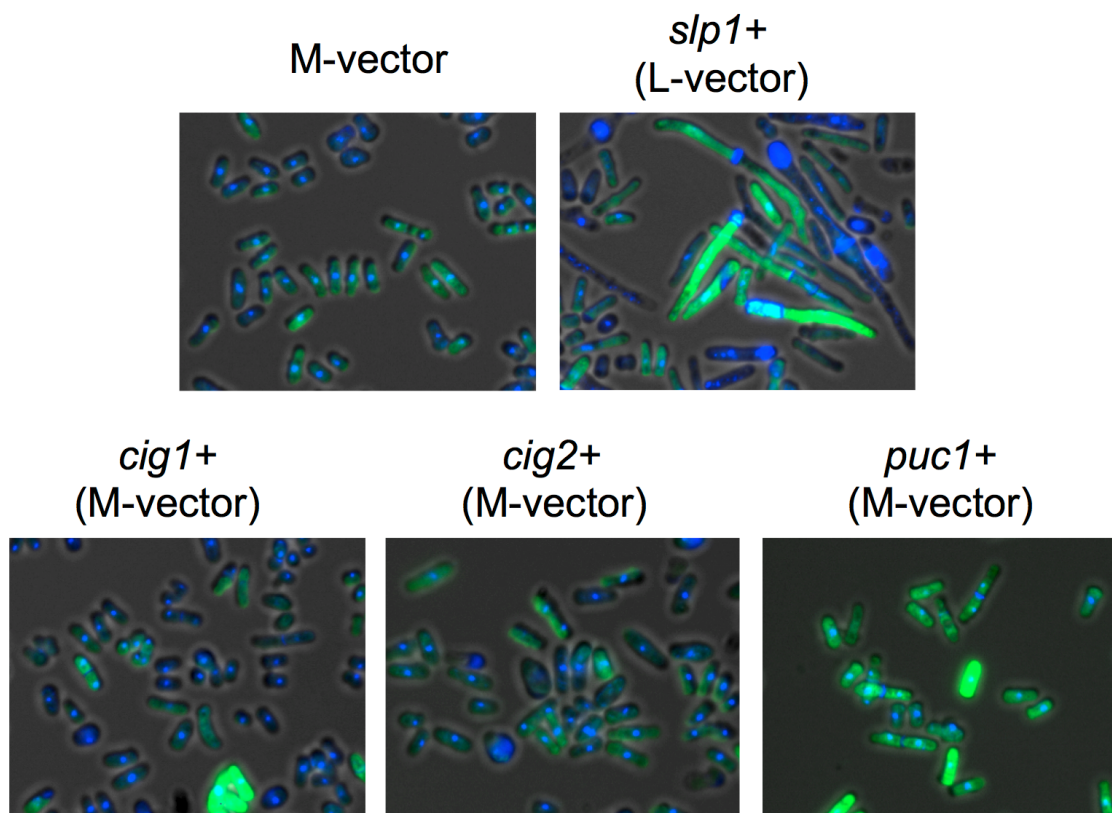


Figure S7. Increased copy numbers of cyclin genes do not give *cdc* phenotype.

Cells harboring pTOW plasmid with the indicated gene were cultured in leucine-condition. GFP fluorescence, nucleus, and septum were observed as shown in Figure 2. *slp1+* is a control gene giving the *cdc* phenotype (elongated cellular morphology).

Table S9. Copy number limits of cell-cycle regulators in the wild type (WT) and cell cycle mutant strains.

Strain ^{*1}	Target Gene	Copy Number (\pm SD) ^{*2}	%/WT	P-value ^{*3}
WT	<i>cdc10+</i>	20.9 \pm 6.2		
WT	<i>cdc13+</i>	1.6 \pm 0.6		
WT	<i>cdc18+</i>	26.2 \pm 4.3		
WT	<i>cdc25+</i>	23.0 \pm 5.8		
WT	<i>cig1+</i>	18.2 \pm 7.7		
WT	<i>cig2+</i>	16.8 \pm 11.1		
WT	<i>clp1+</i>	3.1 \pm 1.4		
WT	<i>mik1+</i>	49.4 \pm 20.3		
WT	<i>puc1+</i>	33.7 \pm 9.6		
WT	<i>rum1+</i>	10.8 \pm 10.3		
WT	<i>slp1+</i>	17.2 \pm 3.7		
WT	<i>srw1+</i>	24.4 \pm 5.5		
WT	<i>wee1+</i>	1.7 \pm 1.3		
WT	<i>pyp3+</i>	41.4 \pm 15.4		
WT	vector	32.0 \pm 11.6		
<hr/>				
<i>cig1Δ</i>	<i>cdc10+</i>	31.7 \pm 7.0	151	5.2E-02
<i>cig1Δ</i>	<i>cdc13+</i>	2.1 \pm 0.4	130	2.7E-01
<i>cig1Δ</i>	<i>cdc18+</i>	36.1 \pm 7.2	138	3.2E-02
<i>cig1Δ</i>	<i>cdc25+</i>	34.2 \pm 8.1	149	4.6E-02
<i>cig1Δ</i>	<i>cig1+</i>	19.1 \pm 18.3	105	9.2E-01
<i>cig1Δ</i>	<i>cig2+</i>	19.3 \pm 8.3	115	6.8E-01
<i>cig1Δ</i>	<i>clp1+</i>	1.9 \pm 0.1	61	8.5E-02
<i>cig1Δ</i>	<i>mik1+</i>	48.4 \pm 11.6	98	9.3E-01
<i>cig1Δ</i>	<i>puc1+</i>	22.8 \pm 11.8	67	1.8E-01
<i>cig1Δ</i>	<i>rum1+</i>	2.4 \pm 0.9	22	1.4E-02
<i>cig1Δ</i>	<i>slp1+</i>	14.3 \pm 11.3	83	5.7E-01
<i>cig1Δ</i>	<i>srw1+</i>	54.7 \pm 23.1	224	1.1E-02
<i>cig1Δ</i>	<i>wee1+</i>	1.1 \pm 0.2	62	4.3E-01
<i>cig1Δ</i>	<i>pyp3+</i>	51.8 \pm 9.9	125	2.3E-01
<i>cig1Δ</i>	vector	51.1 \pm 5.3	160	1.2E-01
<hr/>				
<i>clp1Δ</i>	<i>cdc10+</i>	15.5 \pm 0.3	74	1.9E-01
<i>clp1Δ</i>	<i>cdc13+</i>	2.5 \pm 0.4	155	7.0E-02

<i>clp1Δ</i>	<i>cdc18+</i>	29.0 ± 7.3	111	2.1E-01
<i>clp1Δ</i>	<i>cdc25+</i>	20.5 ± 2.5	89	5.2E-01
<i>clp1Δ</i>	<i>cig1+</i>	8.6 ± 5.7	47	1.0E-02
<i>clp1Δ</i>	<i>cig2+</i>	11.0 ± 4.0	65	4.2E-01
<i>clp1Δ</i>	<i>clp1+</i>	2.5 ± 0.5	81	5.1E-01
<i>clp1Δ</i>	<i>mik1+</i>	24.3 ± 3.6	49	8.5E-02
<i>clp1Δ</i>	<i>puc1+</i>	25.7 ± 13.5	76	2.6E-01
<i>clp1Δ</i>	<i>rum1+</i>	6.8 ± 1.2	63	5.3E-01
<i>clp1Δ</i>	<i>slp1+</i>	3.0 ± 2.1	18	9.0E-06
<i>clp1Δ</i>	<i>srw1+</i>	17.0 ± 13.5	70	2.4E-01
<i>clp1Δ</i>	<i>wee1+</i>	1.2 ± 0.7	72	5.8E-01
<i>clp1Δ</i>	<i>pyp3+</i>	26.8 ± 4.1	65	1.6E-01
<i>clp1Δ</i>	vector	19.6 ± 4.9	61	1.3E-01

<i>puc1Δ</i>	<i>cdc10+</i>	20.3 ± 23.0	97	9.5E-01
<i>puc1Δ</i>	<i>cdc13+</i>	1.9 ± 0.3	121	4.3E-01
<i>puc1Δ</i>	<i>cdc18+</i>	37.0 ± 6.7	141	1.2E-02
<i>puc1Δ</i>	<i>cdc25+</i>	48.8 ± 18.4	212	8.4E-03
<i>puc1Δ</i>	<i>cig1+</i>	21.7 ± 17.4	119	6.7E-01
<i>puc1Δ</i>	<i>cig2+</i>	14.9 ± 9.9	89	7.8E-01
<i>puc1Δ</i>	<i>clp1+</i>	2.8 ± 0.5	92	7.0E-01
<i>puc1Δ</i>	<i>mik1+</i>	51.7 ± 11.9	105	8.3E-01
<i>puc1Δ</i>	<i>puc1+</i>	30.7 ± 7.1	91	6.4E-01
<i>puc1Δ</i>	<i>rum1+</i>	7.0 ± 1.0	64	5.5E-01
<i>puc1Δ</i>	<i>slp1+</i>	13.9 ± 7.2	81	3.8E-01
<i>puc1Δ</i>	<i>srw1+</i>	65.5 ± 23.1	268	2.1E-03
<i>puc1Δ</i>	<i>wee1+</i>	1.5 ± 0.3	87	7.9E-01
<i>puc1Δ</i>	<i>pyp3+</i>	56.3 ± 21.3	136	2.6E-01
<i>puc1Δ</i>	vector	53.5 ± 20.4	167	7.7E-02

<i>srw1Δ</i>	<i>cdc10+</i>	20.4 ± 4.7	97	8.9E-01
<i>srw1Δ</i>	<i>cdc13+</i>	0.7 ± 0.1	44	5.2E-02
<i>srw1Δ</i>	<i>cdc18+</i>	23.1 ± 3.0	88	8.2E-01
<i>srw1Δ</i>	<i>cdc25+</i>	0.3 ± 0.1	1	2.5E-06
<i>srw1Δ</i>	<i>cig1+</i>	20.6 ± 12.8	113	7.2E-01
<i>srw1Δ</i>	<i>cig2+</i>	16.3 ± 12.0	97	9.5E-01
<i>srw1Δ</i>	<i>clp1+</i>	1.4 ± 1.1	45	1.1E-01
<i>srw1Δ</i>	<i>mik1+</i>	27.3 ± 4.4	55	1.2E-01

<i>srw1Δ</i>	<i>puc1+</i>	35.1 ± 17.8	104	8.8E-01
<i>srw1Δ</i>	<i>rum1+</i>	4.6 ± 2.9	43	3.5E-01
<i>srw1Δ</i>	<i>slp1+</i>	12.5 ± 3.2	73	1.1E-01
<i>srw1Δ</i>	<i>srw1+</i>	24.0 ± 3.0	98	9.1E-01
<i>srw1Δ</i>	<i>wee1+</i>	1.0 ± 0.4	56	3.7E-01
<i>srw1Δ</i>	<i>pyp3+</i>	20.7 ± 1.6	50	6.0E-02
<i>srw1Δ</i>	vector	12.7 ± 2.9	40	2.9E-02

*1 For WT, *clp1Δ*, *cig1Δ*, *puc1Δ*, and *srw1Δ* strains, haploid progenies of BG_0000, BG_0465, BG_4780, BG_4172, and BG_0289 (Bioneer) were used, respectively.

*2 Copy numbers were determined using pTOWsp-M vector.

*3 P-value of the two-tailed student t-test against wild type.

Supplementary model description and simulation results

6. Mathematical models of fission yeast cell cycle

In this supplement we present three models for the fission yeast cell with increasing complexity. The core model has been developed for describing DNA replication control based on our previous model for the fission yeast cell cycle (Novak et al., 2001; Sveiczer et al., 2004). This ‘core model’ developed independently of the gTOW experimental data gave amazingly good estimates for upper gene dosage limits. Since not all the cell cycle regulators tested in the gTOW experiments were represented in the core model, we have decided to expand this core model by incorporating the missing cell cycle regulators. None of these two models take into account the level of Cdc2 kinase that thought to be present in excess. Since the gTOW data suggested that Cdc2 level has an influence on upper gene dosage limits of cyclins, we have taken into account the complex formation between cyclin and Cdc2 in a third model.

6.1 A model for DNA replication regulation (“basic model”)

A recently published paper from Nurse’s lab (Hermand and Nurse, 2007) has shown that the licensing factor, Cdc18 is necessary for the DNA replication checkpoint in fission yeast. If the process of DNA replication is compromised, Cdc18 inactivates the S-phase Cdk, Cdc2/Cig2 and the M-phase Cdk, Cdc2/Cdc13 through Rad3 dependent Tyr-phosphorylation mechanism (Rhind and Russell, 1998; Zarzov et al., 2002). We have built a mathematical model to investigate how Cdc18 can fulfill its checkpoint function in various mutant cells based on the networks shown on Figure S8 and Figure S9. In session 8 we present the details of this model, what we refer later as the “*basic model*”.

6.2 Models to investigate gTOW experiments

The first model was a slightly modified version of the previous ‘core model’ in order to describe the gTOW experimental data. Our goal was to show the upper limit of the overexpressed proteins *in silico*. For this reason the ‘core model’ was extended with other important cell cycle regulatory components such as Clp1, Cig1 and Puc1 (see Figure S8, red coloured molecules and regulatory connections). We were able to simulate different types of gTOW induced viability losses (see Figure S11 and Figure S12) as well as almost 42 already published mutant behaviors (see Table S10). We also checked how the deletion of cell cycle regulators affects gTOW experimental results in a “2 dimensional gTOW” simulation (see Table S11). This model will be presented in chapter 9 and will be referred as the “*gTOW model*”.

Our last goal was to test the competition of four possible cyclins (Cdc13, Cig1, Cig2 and Puc1) in binding the fission yeast cyclin dependent kinase, Cdc2 (see

Table S12). This analysis has required a slight modification of the model (see Figure S8, green coloured molecules and regulatory connections). These additions are described in chapter 10 and the extended model is called the “*Cdc2-level model*”.

7. Description of the regulatory interactions of cell cycle control network

Here we present the basic principles of fission yeast cell cycle regulation and describe the details of the ‘core model’.

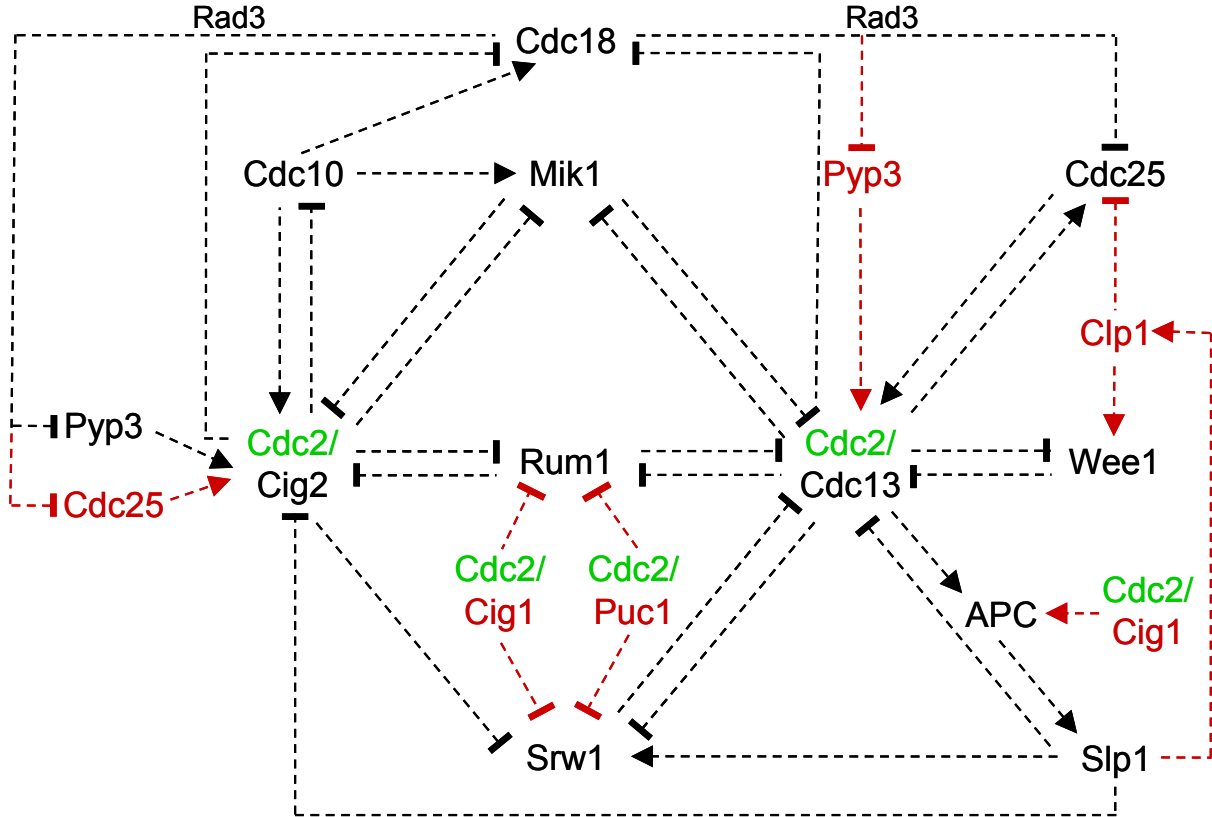


Figure S8. Regulatory interactions among cell cycle regulators in the fission yeast cell cycle control network.

Arrows and blocked end lines represent stimulation of synthesis (or activation) and repression of synthesis (or inhibition). Black letters and arrows represent components and interaction in the original “basic model”. Red colours show the additions to the “gTOW model”, while the green Cdc2 signs show that Cdc2 explicitly appears only in the extended “Cdc2-level model”.

Cdc10 mediated transcription requires the activation of necessary genes to enter the S phase in fission yeast. Cdc10 is the transcriptional activator for Cdc18 (Kelly et al., 1993), Cig2 (Ayte et al., 2001) and Mik1 (Ng et al., 2001). The transcription factor turns on at mitosis and it is active all over G1 phase of the cell cycle (Baum et al., 1997).

The appearing S-phase cyclin, Cig2 binds to Cdc2 kinase. Cdc2 is thought to be not rate limiting for Cdc2/Cig2 complex formation. As a consequence the amount of the complex depends only on cyclin level. The Cdc2/Cig2 complex cannot be active in G1 phase, because a stoichiometric inhibitor (Rum1) binds to it and inhibits its activity. However Rum1 is only present in G1, because at G1/S transition Rum1 is down-regulated by Cdks. Both Cdc2/Cig2 and Cdc2/Cdc13 can phosphorylate Rum1 and thereby promote its degradation by proteasome after SCF-dependent ubiquitination (Benito et al., 1998). Therefore Cdc2/Cig2 and Rum1 have an antagonistic relationship (Martin-Castellanos et al., 1996; Labib and Moreno, 1996), and Cdc2/Cig2 is released from the Rum1 inhibition at the end of G1 phase. After the activation of Cdc2/Cig2, a negative feedback loop is operating, because the active Cdc2/Cig2

can inactivate Cdc10, its own transcription factor (Ayte et al., 2001; McInerny et al., 1995). Cig2 is degraded by ubiquitin-mediated proteolysis (with APC and SCF as ubiquitin-ligases). At the end of mitosis and during early G1 phase APC/Slp1 destroys Cdc2/Cig2 activity, while SCF regulates the kinase activity during S, G2 and M phases (Yamano et al., 2004). Cdc2/Cig2 is also regulated by Tyr-phosphorylation (Hermand & Nurse). We propose that Mik1 kinase is responsible for Cdc2/Cig2 phosphorylation dependent inhibition (see later). In the model Cdc2/Cig2 also has negative effect on Mik1 in two different ways: Cdc2/Cig2 inhibits Cdc10, the transcription factor of Mik1, and promotes degradation of Mik1 (by phosphorylating and targeting it for SCF mediated ubiquitination). Having been inactivated by Tyr-phosphorylation, Cdc2/Cig2 requires Tyr-phosphatases, which can activate the complex. These phosphatases might be Cdc25 and Pyp3. Cig2 has a role to down-regulate mitotic kinase inhibitors, such as Rum1 and Srw1/APC thereby it helps entering into the cycle (Kominami et al., 1998). However, Cig2 is not essential protein and *cig2Δ* cells behave like wild type cells (Bueno and Russell, 1993).

The temporal pattern of the mitotic kinase, Cdc2/Cdc13 activity is complex: zero in G1, appears at Start, low during S/G2 phase and high in M phase and drops at mitotic exit (Nurse, 1999). The Cdc2/Cdc13 activity is regulated by many different ways, which has been described by our previous models (Novak et al., 2001; Sveiczer et al., 2004) therefore we summarize this part of the model very briefly. There is an antagonistic relationship between Cdc2/Cdc13 and its enemies Rum1 and APC/Srw1 in G1 phase. Overcoming its enemies, Cdc2/Cdc13 activity is regulated by Cdc25 and Pyp3 phosphatases and Wee1 and Mik1 kinases in G2 phase. Wee1 and Mik1 inactivate Cdc2/Cdc13 by Tyr-phosphorylation, while Cdc25 and Pyp3 can remove the inhibitory phosphate group. We propose that Cdc2/Cdc13 promotes Mik1 degradation; it inhibits Wee1 and activates Cdc25. After turning off the inhibitory effect of Wee1 and Mik1 kinases a sharp increase of Cdc2/Cdc13 activity occurs at the G2/M transition. After mitosis Cdc2/Cdc13 activates APC/Slp1, followed by APC/Srw1, which promote the ubiquitin dependent degradation of Cdc13. While there is a double negative feedback between Cdc2/Cdc13 and Srw1/APC, Slp1/APC is activated by a time-delayed negative feedback loop (Correa-Bordes and Nurse, 1995; Morgan, 1999; Nurse, 1990; Peters, 2002; Sveiczer et al., 2004).

The licensing factors are essential for the initiation and for the proper control of DNA replication during the cell cycle. One of the licensing factors is called Cdc18 in fission yeast. Cdc18 deleted cells are inviable (see Figure S10) (Kelly et al., 1993; Nishitani and Nurse, 1995). Cdc18 is expressed all over G1 and S phases of the cell cycle. The presence of Cdc18 in S phase cells suggest that the block of re-replication mechanism operates down-stream of Cdc18. Cdc18 disappears in G2 and M phases of the cycle for two reasons. Its transcription factor (Cdc10) gets inhibited by Cdc2/Cig2 (see above) and it is rapidly degraded by Cdk phosphorylation dependent proteolysis. Both Cdc2/Cig2 and Cdc2/Cdc13 phosphorylate Cdc18 and target it for degradation by SCF. SCF is required for degradation of Cdc18 after the S phase (Brown et al., 1997; Kominami and Toda, 1997; Lopez-Girona et al., 1998). The degradation of the Cdc18TA protein with non-phosphorylatable Cdk phosphorylation sites is compromised and it creates a G2 block (see Figure S10) (Jallepalli et al., 1997).

Checkpoints mechanisms are important during cell cycle progression in response to e.g. DNA damage or DNA replication defect. Checkpoint mechanisms delay further cell cycle progression and thereby they are making it possible to repair DNA lesions; compromised checkpoint functions could lead to loss of genome stability. Blocked DNA replication generates an inhibitory signal that blocks initiation of mitosis. A central component of this

checkpoint pathway is Rad3 protein-kinase (Bentley et al., 1996; Carr, 1995). Rad3 is required to initiate and to maintain DNA replication checkpoint, but it is necessary only to initiate DNA damage checkpoint (Humphrey, 2000). Both Cdc2/Cig2 and Cdc2/Cdc13 are targets of the DNA replication checkpoint mechanism through inhibitory Tyr-phosphorylation (Rhind and Russell, 1998). If the checkpoint is active, Cig2 accumulates to a level higher than normal but the Cdc2/Cig2 complex is kept inactive because of inhibitory Tyr-phosphorylation (Hermand and Nurse, 2007; Zarzov et al., 2002). Therefore during an S-phase block, the Tyr-phosphatases (Cdc25 and Pyp3) might be inhibited, while the Tyr-kinases (Mik1) should be activated. Recent experiments from the Nurse's lab suggest that Cdc18 is required for proper checkpoint control. In a checkpoint block, Cdc18 protein level is high which keeps the Cdks in an inactive Tyr-phosphorylated form through Rad3 pathway (Hermand and Nurse, 2007).

7.1. Methods to construct a mathematical model of fission yeast cell cycle

The chemical reactions of the interacting molecules were translated into forms of differential equations by standard principles of biochemical kinetics and a set of ordinary differential equations (ODEs) were created. The differential equations have been solved numerically. For simulation a freely available computer program XPP-AUT were used, from G. Bard Ermentrout at Department of Mathematics, University of Pittsburgh (<http://www.math.pitt.edu/~bard/xpp/xpp.html>).

All variables are dimensionless and represent relative protein concentrations. Thus all reaction rates have a dimension of 1/min. We do not consider cell growth and size control in this model therefore our model is a simple limit cycle oscillator. Our goal was to test how the overexpression of different cell cycle regulators influences the temporal pattern of oscillation. We set the kinetic parameters to get a 90 min long cell cycle (period) time for wild type cells.

Cell size differences we approximate from the maximal values that Cdc13 level reaches during the cell cycles of various mutant simulations.

7.2 Equations and parameters of the models

For the simulations and analyses three .ode files were used:

1. DNArep1_model.ode: this model was created to explain Hermand and Nurse's experimental results (Hermand and Nurse, 2007) about the role of Cdc18 in DNA replication checkpoint,
2. gTOW_model.ode: slightly modified version of DNArep1_model.ode, extended with new components: Clp1, Cig1, Puc1 and fitted to gTOW results,
3. Cdc2_model.ode: extended version of gTOW_model.ode with Cdc2 and Cdc2/cyclin complex formation.

The .ode files can be simulated by XPP-AUT. The files contain the initial conditions and parameter values of the components and settings for simulating wild type behavior.

8. The “basic model” (core model)

Here we describe the details of the DNA replication control in our model, together with the most important simulation results.

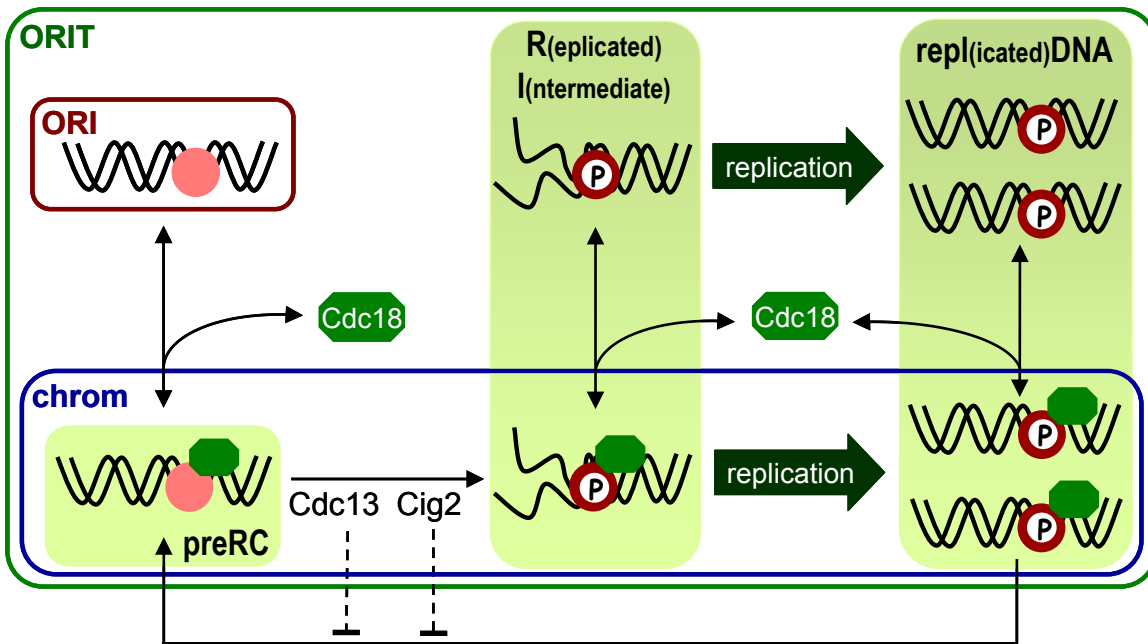


Figure S9. Different forms of DNA replication origins in the model.

The pink circle represents the ORI complex at replication origins where Cdc18 (green rectangle) binds to and loads MCM proteins.

Cdc18 protein exists in free (Cdc18f) and chromatin (chrom) bound forms. Cdc18 binds to replication origins that can be in one of the following states depending on their replication states: unreplicated, replicating and replicated. Cdc18 can bind to all of these forms reversibly therefore six different forms can be distinguished, which can be transformed into each other (see the figure). The complex of unreplicated origin with Cdc18 is called preRC. The preRC is transformed into Replication Intermediate (RI) by Cdk dependent phosphorylation during DNA replication. However origins without Cdc18 cannot be activated, because the licensing factor loads necessary replication proteins onto the chromatin (e.g. MCM's). The rate-limiting step for initiation of DNA replication is the appearance of Cdk activity rather than Cdc18.

The replication process (RI into replicated DNA) is described simply by first order reaction. The conversion of replicating and replicated origins back to unreplicated ones is inhibited by Cdks and it can only take place after mitosis when Cdk activities disappear. This mechanism guarantees that there is ‘one and only one S phase’ per cell cycle and blocks re-licensing during G2 and M phases. Cdks target Cdc18 for degradation (not shown on this figure) and the Cdc18T (which is the sum of all the Cdc18 forms) is described by the following differential equation in the model:

$$dCdc18t/dt = (V_{sc18}) - (V_{dc18} * Cdc18t)$$

where

```
Vsc18=ksc18+ksc1810*Cdc10
Vdc18=kdc18+kdc1813*Cdc13+kdc18c2*Cig2+kdc18c2_*pCig2
```

The total amount of chromatin bound Cdc18 is calculated for steady state (assuming fast equilibrium binding between Cdc18 and replication origins):

```
BB=orit+Cdc18t+(ko18r+Vdc18)/ko18
chrom=2.0*orit*Cdc18t/(BB+(BB^2.0-4.0*orit*Cdc18t)^(1.0/2.0))
```

The free Cdc18 is calculated by conservation equation:

```
Cdc18f = Cdc18t - chrom
```

The differential equations of RI (middle column) and replDNA (last column) could be written as follows:

```
dRI/dt=(kini13*Cdc13+kinici2*Cig2+kinici2_*pCig2)*preRC-(krepl*RI)
dreplDNA/dt=(krepl*RI)-(kori/(1.0+((kipre13*Cdc13+kipreci2*Cig2)/Jipre)^n)*replDNA)
```

The concentration of preRC is computed with algebraic equation by assuming again a fast complex formation between free Cdc18 and free ORI:

```
preRC=(orit-RI-replDNA)*Cdc18f/((ko18r+Vdc18)/ko18+Cdc18f)
```

The checkpoint function is represented by Unreplicated DNA (UDNA), which depends on Cdc18 level, the DNA replication state and Rad proteins. Cdc18 is an important checkpoint protein because the replication checkpoint does not work without Cdc18. The Rad3 parameter is one in WT cells, and it is zero in *rad3Δ* cells. The strongest checkpoint signal comes from the replication intermediates in complex with Cdc18 (calculated from RI with equilibrium Cdc18 binding):

```
UDNA=Rad3*(k*Cdc18t+k_p*RI*Cdc18f/((ko18r+Vdc18)/ko18+Cdc18f))
```

When the checkpoint is activated both Cdc2/Cig2 and Cdc2/Cdc13 complexes get Tyr-phosphorylated. Therefore the Tyr-phosphatases (Cdc25 and Pyp3) and Tyr-kinases (Mik1 and Wee1) are the obvious targets of the checkpoint mechanism. In presence of hydroxyurea, cells are blocked in S phase and RI accumulates. RI makes the UDNA signal very strong which blocks the Cdc2/Cig2 - Mik1 bistable switch in the low Cdc2/Cig2 activity state, therefore Cdc2/Cig2 accumulates in Tyr-phosphorylated, inactive forms. As a consequence Cdc2/Cig2 cannot turn off Cdc10, which keeps the protein level of Cdc10 target genes (Cig2, Cdc18 and Mik1) high.

S phase is started when RI starts to accumulate, and it completed when active Cdc2/Cig2 concentration hits a critical value. We assumed the following if replDNA was not dropped below 0.1 then the DNA replication could not be finished properly and the cell not viable due to the re-replication. The replDNA should be dropped close to zero to make possible the proper replication of the chromosomes in the next cycle.

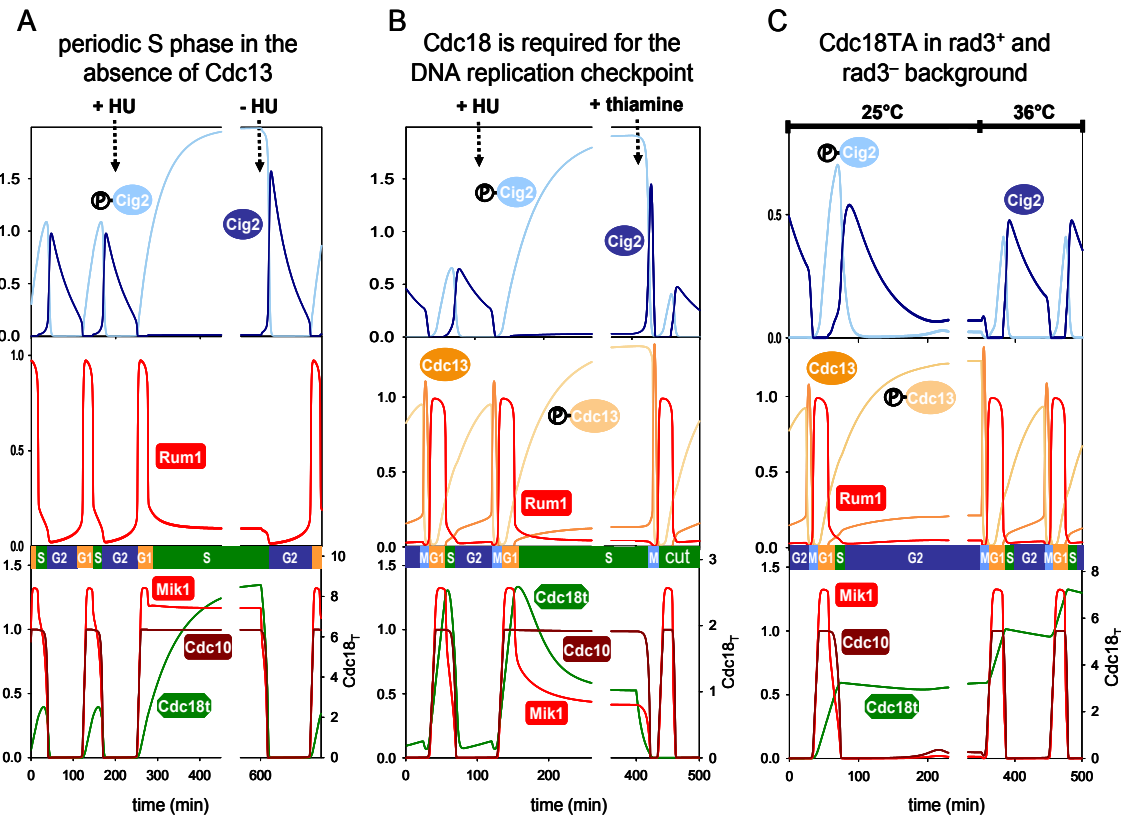


Figure S10. Simulation of Hermand & Nurse experiments with the core model.

On this figure, we illustrate how the core model describes the fundamental experiments of Hermand & Nurse (Hermand and Nurse, 2007).

(A) In one set of experiments the authors were using cdc25 block and release protocol to synchronize cell cycle. Before releasing the G2 arrest caused by inactive cdc25, they shut off the synthesis of Cdc13, the major mitotic cyclin. Under these circumstance, cells undergo synchronous endoreplication cycles (Hayles et al., 1994), which is characterized by oscillation in the activity of S phase cyclin, Cig2. To simulate Cdc13 shut-off, we have set the rate of Cdc13 synthesis (k_{sc13}) to zero. Hydroxyurea (HU) blocks DNA replication by inhibiting one of the required metabolic enzymes. We model the HU block by setting $k_{repl} = 0$ in the equations (at $t = 200$ min) which causes an accumulation of replicating intermediates (RI). HU blocks the endoreplication cycles by activating the checkpoint mechanism and Cdc2/Cig2 accumulates in the Tyr-phosphorylated inactive form. After releasing the DNA replication block (washing out HU, k_{repl} value is set back to the original one at $t = 600$ min) RI gets rapidly transformed to replicated DNA and the DNA replication checkpoint turns off. Cdc2/Cig2 is not inhibited by Rad3, and the complex is dephosphorylated and activated. Thereby Cdc10 mediated transcription turns off and Mik1 and Cdc18 degradation is promoted.

(B) In another experiments Hermand & Nurse turned off Cdc18 synthesis in HU blocked cells, which caused an entry into mitosis without completing DNA replication.

Simulation starts with WT cell cycle and replication is blocked at 100 min by HU (k_{repl} is set to 0). Observe that both Cdc2/Cig2 and Cdc2/Cdc13 complexes are kept inactive by Tyr-phosphorylation because of the DNA replication checkpoint. After Cdc18 synthesis was shut off ($k_{s18} = 0$ at $t = 400$ min), Cdc18 level drops, which compromises the checkpoint, therefore both Cdc2/Cig2 and Cdc2/Cdc13 gets activated. As a consequence cells enter into mitosis although replicating intermediates (RI) are still present. Chromosome segregation of unreplicated DNA creates a ‘cut’ phenotype.

(C) Hermand & Nurse have demonstrated that Cdc18 can activate the checkpoint even without DNA replication intermediates by using a Cdc18 mutant protein (Cdc18TA) in which the Cdk phosphorylation sites were mutated to non-phosphorylatable residues. *Cdc18TA* cells have a higher than normal level of Cdc18 protein because of the compromised degradation of Cdc18. Therefore *Cdc18TA* cells get blocked in G2 phase of the cycle if the checkpoint pathway (e.g. Rad3) is intact. However in the absence of Rad3 activity (*rad3^{ts}* mutants at the restrictive temperature) *Cdc18TA* cells can cycle normally. We have simulated Cdc18TA mutants by setting the Cdc18 degradation rate constant to zero ($k_{dc1813} = 0$, $k_{dc18c2} = 0$ and $k_{dc18c2'} = 0$), which creates a G2 block in the model as well. When the *rad3* parameter was set to zero at 350 min to simulate inactivation of Rad3, normal cell cycles were observed except Cdc18 level increased continuously.

The DNArep1_model.ode file was used for these simulations.

9. The “gTOW model”

The original Basic model was extended by incorporating more cell cycle regulators (red labels on Figure S8) in order to provide a better description of the gTOW experiments.

Newly added component or new connections, compared to the “*basic model*”:

- Both Pyp3 and Cdc25 phosphatases are able to dephosphorylate the Tyr-phosphorylated form of Cdc2/Cig2 and Cdc2/Cdc13 complexes.
- The other two Cdk/cyclin complexes (Cdc2/Cig1 and Cdc2/Puc1) were also incorporated into the model. Cdc2/Cig1 and Cdc2/Puc1 have a role in G1/S transition to promote Rum1 degradation; however Rum1 does not have negative effect on these Cdk/cyclin complexes (Martin-Castellanos et al., 2000; Martin-Castellanos et al., 1996). The kinetic activation of Cig1 is similar to that of Cdc13 (Basi and Draetta, 1995), so Cdc2/Cig1 might have a positive effect on mitotic exit via activating Slp1 indirectly.
- Clp1 phosphatase (also called Flp1) is a homologue of budding yeast Cdc14. Clp1 is activated at mitosis (by Slp1 in this model). Clp1 is able to activate Wee1 kinase and inhibit Cdc25 phosphatase thereby to promote the Tyr-phosphorylation of Cdc2/Cdc13 at the end of mitosis. Thus the deletion of Clp1 shows a semi-wee phenotype, with approximately half the cell size of wild type cells (Trautmann et al., 2001).

9.1. Simulation of gTOW experiments

The mathematical model provides an easy way to simulate the gTOW experiments. We have increased the synthesis rate or the total concentration of different cell cycle regulators in the model up to 256-fold of the normal value and analyzed the temporal pattern of oscillations. The upper limit of gene copy number was set to the highest level of overexpression that still did not change significantly the periodic behavior characteristic for normal cycling. This was performed by hand parameters adjustments. These data are shown in Figure 7B in the main text, where the upper limits of overexpression for 14 regulatory proteins are presented.

These calculations were done by both DNArep1_model.ode (“DNA replication model” in Figure 7B) and gTOW_model.ode (“gTOW model” in Figure 7B). Remember that Cig1, Clp1 and Puc1 are not included in the DNArep1_model.ode):

Studied gene	Modified parameter	
	DNArep1_model	gTOW_model
<i>cdc10+</i>	k_{sc1810} , k_{sci210} , k_{amik10}	T10
<i>cdc13+</i>	k_{sc13}	T8
<i>cdc18+</i>	k_{sc1810}	T12
<i>cdc25+</i>	k_{25_pp}	T7
<i>cig1+</i>	-	T6
<i>cig2+</i>	k_{sci210}	T4
<i>clp1+</i>	-	T2

Studied gene	Modified parameter	
	DNArep1_model	gTOW_model
<i>mik1+</i>	k_{amik10}	T12
<i>puc1+</i>	-	Puc1
<i>pyp3+</i>	k_{pyp}	T0
<i>rum1+</i>	k_{srum}	k_{srum}
<i>slp1+</i>	k_{dc13sl} , k_{dc12sl}	T3
<i>srw1+</i>	k_{dc13sr}	T5
<i>wee1+</i>	k_{wee_pp}	T9

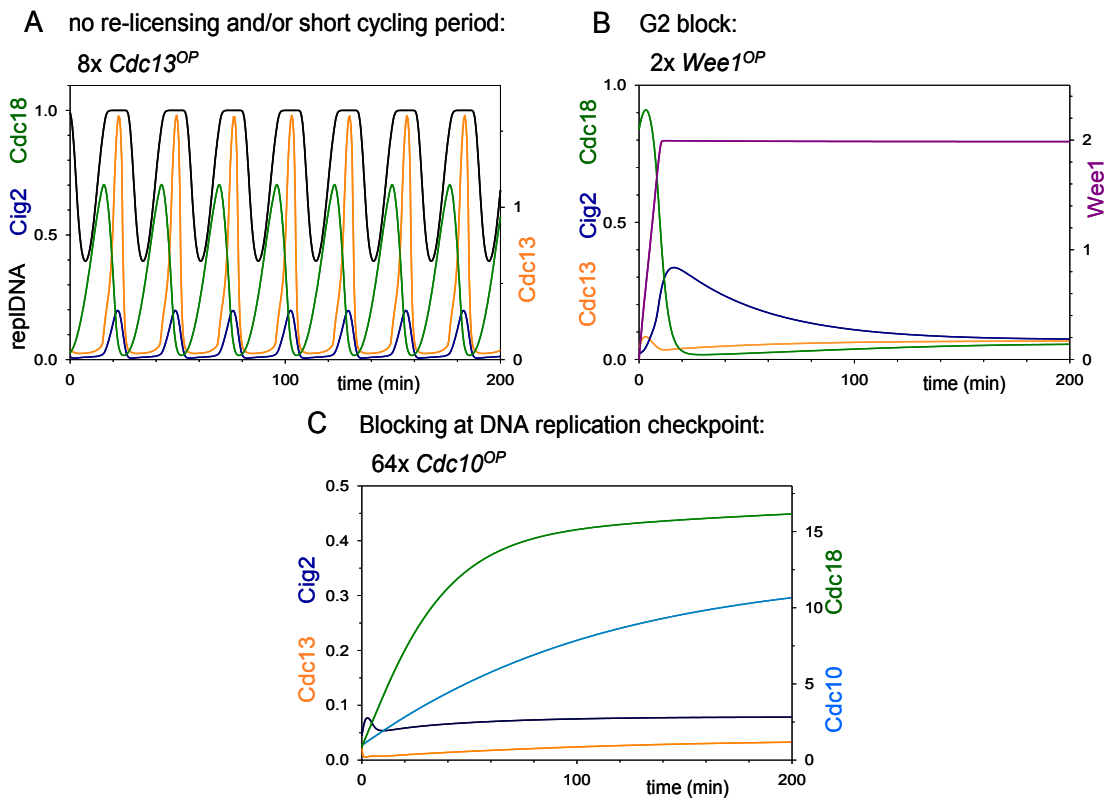


Figure S11. Three different outcomes in gTOW experiments.

(A) No re-licensing and/or short cycling period ($Cdc13^{OP}$, $Cdc25^{OP}$, $Pyp3^{OP}$, $Cig2^{OP}$)

The overexpression of mitotic cyclin, $Cdc13$ is a good example for this mechanism of losing viability. Increasing $Cdc13$ ($k_{sc13} = 0.24$) level reduces the length of the oscillation of the cell cycle. With higher $Cdc13$ level, the cells can enter M phase prematurely. In this case $Cdc2/Cdc13$ can overcome its inhibitory kinases (Mik1 and Wee1) and the length of G2 phase gets shorter. At the very extreme, the cycle gets so short that cells cannot complete DNA replication before division that creates a cut phenotype. The increased level of $Cdc25$ or $Pyp3$ phosphatases also promote early mitotic entry and creates “cut” phenotype at higher level. When $Cig2$ is overexpressed the length of the cell cycle remains the same as in wild type, but the continuously high $Cig2$ level blocks re-licensing of replication origins.

(B) G2 block ($Wee1^{OP}$, $Clp1^{OP}$, $Cig1^{OP}$ and $Slp1^{OP}$)

All of these proteins inhibit the activation of $Cdc2/Cdc13$ by different mechanism, therefore cells cannot enter mitosis if their level is high. Increasing $Wee1$ ($T9 = 2$) protein level keeps the mitotic kinase activity low by inhibitory Tyr-phosphorylation and the cells get blocked in G2 phase with elongated cell size and 2C DNA content. $Clp1$ blocks the cell cycle through $Wee1$ hyper-activation, while $Slp1$ arrests mitotic entry via ubiquitin dependent degradation. High $Cig1$ level activates $Slp1$ prematurely, making impossible the activation of $Cdc2/Cdc13$.

(C) Permanent activation of the DNA replication checkpoint ($Cdc10^{op}$, $Cdc18^{op}$, $Mik1^{op}$)

$Cdc10$ is a typical example for this phenotype. Increasing $Cdc10$ ($T10 = 64$) level leads to an increased protein level of $Cdc10$'s target genes, such as $Cig2$, $Cdc18$ and $Mik1$. Since $Cdc18$ and $Mik1$ are important to activate the DNA replication checkpoint, the cell cycle gets blocked in G2 phase above a critical level of $Cdc10$ with $Cdc2/Cig2$ and $Cdc2/Cdc13$ complexes Tyr-phosphorylated. Similar G2 block happens when $Cdc18$ or $Mik1$ are overexpressed. Our model cannot explain the over-replication phenotype of $cdc18^{op}$ cells.

The gTOW_model.ode file was used for these simulations and the given parameter of the component was changed for overexpression.

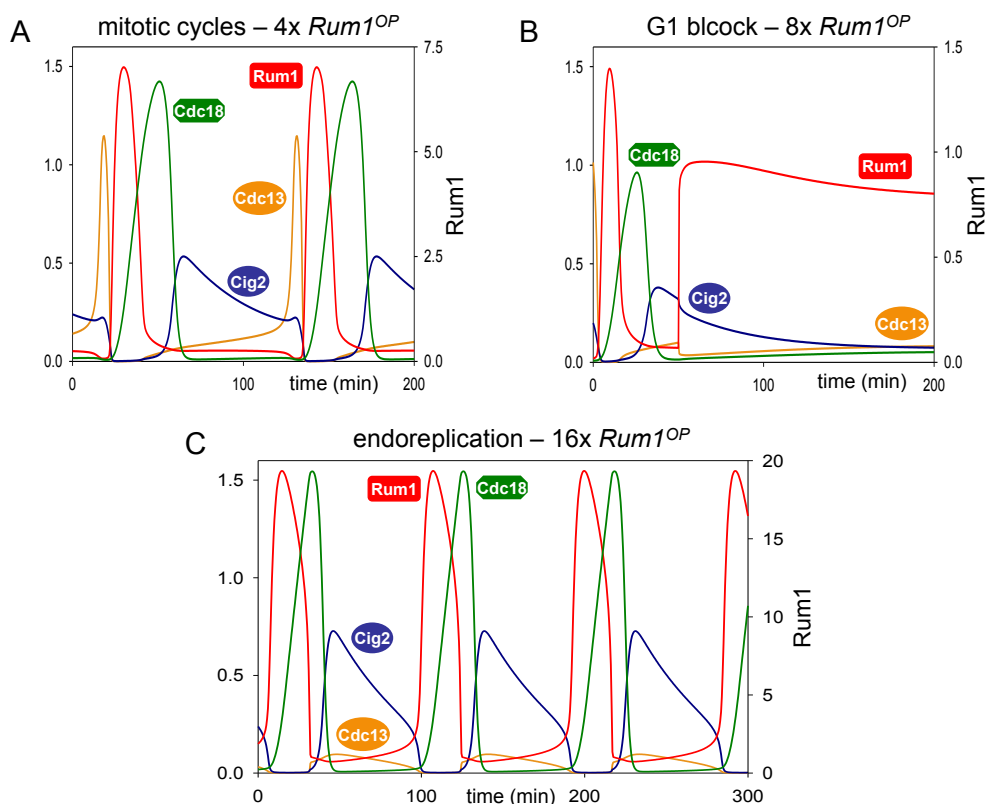


Figure S12. Rum1 overexpression can block mitotic cycle in different way.

We have found that Rum1 overexpression creates different type of temporal patterns in cell cycle regulators depending on its expression level. Four-fold higher than normal level of expression does not interfere with mitotic cycling (see panel A). However 8-fold expression creates a G2 block, because Rum1 binds to and inhibits both $Cdc2/Cig2$ and $Cdc2/Cdc13$ complexes (panel B). This terminal phenotype is consistent with the gTOW experimental data presented in this paper. However a 16-fold Rum1

overexpression converts the mitotic cycle into an endoreplication cycle in the model (panel C). Actually, the Rum1 gene has been discovered by the amplified DNA content of Rum1 overexpression, which is the consequence of endoreplication cycles (Moreno and Nurse, 1994).

Rum1 is a stoichiometric inhibitor of Cdk/cyclin complexes, but the strength of the inhibition (K_d values) are different for different complexes (Correa-Bordes and Nurse, 1995). Since Rum1 is the best inhibitor of the Cdc2/Cdc13 complexes, therefore G2 block is the first terminal phenotype with increasing Rum1 level. In order to convert the G2 block into an endoreplication cycle, Cdc2/Cig2 activity has to be down-regulated. Since Rum1 is a weaker inhibitor for the Cdc2/Cig2 complex than for Cdc2/Cdc13, endoreplication cycle requires a higher level of Rum1 expression.

The gTOW_model.ode file was used for these simulations and the synthesis rate of the Rum1 ($k_{srum} = 4, 8$ and 16 respectively) was changed for overexpression.

The gTOW model can simulate not only the gTOW experiments (see Figure 7B in main text) but also able to explain the mutants of DNA replication (see above) as well as many other mutant phenotypes. These mutants were created using gTOW_model.ode file. The parameter changes, the mutants' phenotypes and references are also shown in the Table S10. **Investigated mutant phenotypes.** The maximum values of Cdc13total at periodic cycles and the re-licensing capability of the mutants are also detailed in separated columns. These features are crucial to determine the different mutant behavior of the cell. The column "comment" shows whether the model predicts a phenotype consistent with experimental observations ("OK") or not.

Table S10. Investigated mutant phenotypes.

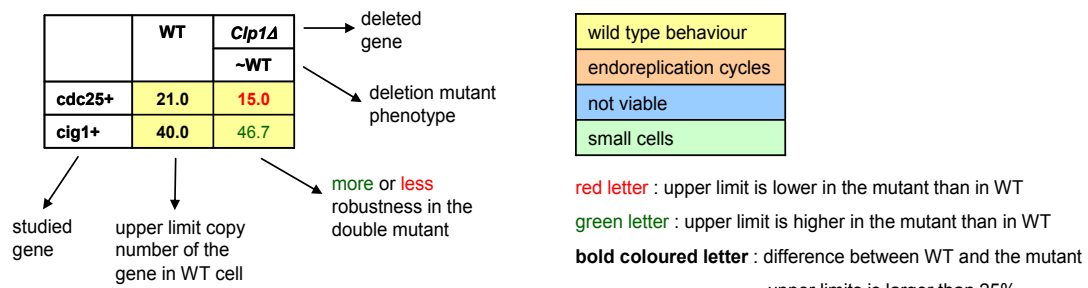
Mutants	Parameter changes	Phenotype	References	Cdc13max at periodic cycles	Re-license	Comment
wild type (WT)	-	WT	-	1.15	yes	OK
<i>wee1ts</i>	T9=0.15	semi-WT	Nurse and Thuriaux, 1980	0.57	yes	OK
<i>wee1Δ</i>	T9=0	semi-WT	Nurse and Thuriaux, 1980	0.63	yes	OK
<i>mik1Δ</i>	T12=0	nearly WT	Lundgren et al., 1991	1.15	yes	OK
<i>mik1Δ</i> <i>wee1ts</i>	T12=0, T9=0.15	cut	Lundgren et al., 1991	0.58	no	OK
<i>mik1Δ</i> <i>wee1ts</i> <i>cig2Δ</i>	T12=0, T9=0.15, T4=0	semi-WT	Bueno and Russell, 1993	0.58	yes	OK
<i>pyp3Δ</i>	T0=0	nearly WT	Millar et al., 1992	1.34	yes	OK
<i>cdc25ts</i>	T7=0.1	G2 block	Russell and Nurse, 1986	-	no	OK
<i>cdc25Δ</i>	T7=0	G2 block	Russell and Nurse, 1986	-	no	OK
<i>wee1ts</i> <i>cdc25Δ</i>	T9=0.15, T7=0	quantized cycles	Sveiczer et al., 1996	0.70	no	low amplitude

						oscillator
<i>wee1ts</i>	T9=0.15, T7=0.1	semi-wee1	Grallert et al., 1998	0.63	yes	OK
<i>wee1Δ</i>	T9=0, T7=0	semi-wee1	Sveiczer et al., 2000	0.57	yes	OK
<i>wee1ts</i> <i>cdc25Δ</i> <i>mik1Δ</i>	T9=0.15, T7=0, T12=0	quantized cycles	Lundgren et al., 1991	0.70	no	low amplitude oscillator
<i>cig1Δ</i>	T6=0	nearly WT	Bueno and Russell, 1993	1.15	yes	OK
<i>cig2Δ</i>	T4=0	nearly WT	Bueno and Russell, 1993	1.33	yes	OK
<i>cig1Δ</i> <i>cig2Δ</i>	T4=0, T6=0	nearly WT	Martin-Castellanos et al., 1996	1.33	yes	OK
<i>puc1Δ</i>	Puc1=0	nearly WT	Forsburg and Nurse, 1994	1.14	yes	OK
<i>cig1Δ</i> <i>wee1ts</i>	T6=0, T9=0.15	semi-WT	Bueno and Russell, 1993	0.56	yes	OK
<i>cig2Δ</i> <i>wee1ts</i>	T4=0, T9=0.15	semi-WT	Bueno and Russell, 1993	0.56	yes	OK
<i>cig1Δ</i> <i>cig2Δ</i> <i>wee1ts</i>	T4=0, T6=0, T9=0.15	semi-WT	Martin-Castellanos et al., 2000	0.56	yes	OK
<i>puc1Δ</i> <i>wee1ts</i>	T0=0, T9=0.15	semi-WT	Martin-Castellanos et al., 2000	0.58	yes	OK
<i>rum1Δ</i>	ksrum=0	nearly WT	Moreno and Nurse, 1994	1.10	yes	OK
<i>rum1Δ</i> <i>cig2Δ</i>	ksrum=0, T4=0	nearly WT	Martin-Castellanos et al., 1996	1.29	yes	OK
<i>rum1Δ</i> <i>wee1ts</i>	ksrum=0, T9=0.15	too small	Moreno and Nurse, 1994	0.58	no	OK
<i>srw1Δ</i>	T5=0	nearly WT	Kitamura et al., 1998	1.17	yes	OK
<i>srw1Δ</i> <i>cig2Δ</i>	T5=0, T4=0	nearly WT	Kitamura et al., 1998	1.38	yes	OK
<i>srw1Δ</i> <i>wee1ts</i>	T5=0, T9=0.15	too small	Kitamura et al., 1998	0.59	no	OK
<i>srw1Δ</i> <i>rum1d</i>	T5=0, ksrum=0	nearly WT	Yamaguchi et al., 2000	1.11	yes	OK
<i>srw1Δ</i> <i>rum1Δ</i> <i>wee1ts</i>	T5=0, ksrum=0, T9=0.15	too small	Sveiczer et al., 2000	0.56	no	OK
<i>srw1Δ</i> <i>mik1Δ</i>	T5=0, T12=0	nearly WT	Kitamura et al., 1998	1.18	yes	OK
<i>slp1ts</i>	T3=0.01	M block	Kim et al., 1998	-	no	OK
<i>clp1Δ</i>	T2=0	smaller than WT	Trautmann et al., 2001	1.10	yes	OK
<i>clp1Δ</i> <i>wee1ts</i>	T2=0, T9=0.15	semi-WT	Trautmann et al., 2001	0.58	yes	OK
<i>cdc13Δ</i>	ksc13=0	endoreplicati on	Hayles et al., 1994	-	yes	OK
<i>cdc13Δ</i> <i>cig1Δ</i>	ksc13=0, T6=0	endoreplicati on	Mondesert et al., 1996	-	yes	OK
<i>cdc13Δ</i> <i>cig2Δ</i>	ksc13=0, T4=0	G1 block	Mondesert et al., 1996	-	no	OK
HU	krepl=0	S block	Enoch et al., 1992	-	no	OK
<i>cdc13Δ</i> HU	ksc13=0,	S block	Zarzov et al., 2002	-	no	OK

	krepl=0					
<i>cdc18Δ</i>	ksc1810=0, ksc18=0	cut	Kelly et al., 1993	1.15	no	OK
<i>cdc18Δ HU</i>	ksc1810=0, ksc18=0, krepl=0	cut	Hermand and Nurse, 2007	1.15	no	OK
<i>rad3Δ</i>	Rad3=0	nearly WT	Martinho et al., 1998	1.15	yes	OK
<i>rad3Δ HU</i>	Rad3=0 krepl=0	cut	prediction	1.15	no	OK
<i>cdc18TA</i>	kdc1813=0, kdc18c2=0, kdc18c2'=0	G2 block	Hermand and Nurse, 2007	-	no	OK
<i>cdc18TA</i> <i>rad3Δ</i>	kdc1813=0, kdc18c2=0, kdc18c2'=0, Rad3=0	nearly WT	Hermand and Nurse, 2007	1.15	yes	OK

Table S11. Testing gTOW in single deletion mutants *in silico*.

	WT	<i>Cdc10Δ</i>	<i>Cdc13Δ</i>	<i>Cdc18Δ</i>	<i>Cdc25Δ</i>	<i>Cig1Δ</i>	<i>Cig2Δ</i>	<i>Clp1Δ</i>	<i>Mik1Δ</i>	<i>Puc1Δ</i>	<i>Pyp3Δ</i>	<i>Rum1Δ</i>	<i>Slp1Δ</i>	<i>Srw1Δ</i>	<i>Wee1Δ</i>	
	G1 block	endorepl.	cut	G2 block	~WT	~WT	~WT	~WT	~WT	~WT	~WT	~WT	M block	~WT	~0.5*WT	
<i>cdc10+</i>	61.0		1.0				1.0		22.0	53.0	2.0			65.0	256.0	
<i>cdc13+</i>	6.7				2.3-8.7				6.0				2.3		3.7	5.7
<i>cdc18+</i>	62.0		1.0				1.0		86.0	50.0	2.0	64.0		70.0	256.0	
<i>cdc25+</i>	21.0		38.0				256.0	15.0	14.0	256.0	41.0	8.0		12.0	10.0	
<i>cig1+</i>	40.0		20.0				26.6	46.7			30.0				4.0	
<i>cig2+</i>	23.0		1.0					22.0	15.0	24.0	28.0	7.0		17.0	1.0	
<i>clp1+</i>	6.0		256.0				2.0		7.0	5.0	3.0	7.0		8.0	256.0	
<i>mik1+</i>	22.0		1.0				10.0	27.0		12.0	6.0	24.0		35.0	124.0	
<i>puc1+</i>	256.0		9.0						140.0						1.0	
<i>pyp3+</i>	240.0		1.0				256.0	198.0	235.0	220.0		8.0		21.0	2.0	
<i>rum1+</i>	7.0		3.0		9.0-33.0		2.0			5.0	6.0		12.0-35.0	8.0	1.0	
<i>slp1+</i>	31.0		256.0				7.0	39.0	32.0	27.0	11.0	39.0		37.0	3.0	
<i>srw1+</i>	92.0		256.0			93.0	21.0	115.0	95.0	81.0	31.0	117.0			15.0	
<i>wee1+</i>	1.3		256.0				1.0	1.4	1.4	1.2	1.1	1.4			1.4	



A systematic analysis was done to test the robustness of the system for these gTOW overexpressions. The main regulatory proteins were deleted one by one and we studied how the upper limits of the other proteins' overexpression are changing, managing a 2 dimensional gTOW analysis in fission yeast *in silico*.

Some mutant combinations cannot be performed at all, because the deletion of the protein such as Cdc10 (Ayte et al., 2001), Cdc13 (Hayles et al., 1994), Cdc18 (Kelly et al., 1993), Cdc25 (Russell and Nurse, 1986) and Slp1 (Kim et al., 1998) creates inviable phenotype (blue background). The G1 block of Cdc10 could not be simulated, which assumes an unknown blocking mechanism of cell cycle at the absence of transcription factor. *Cdc25Δ* is inviable, because Cdc13 cannot be activated and the cells cannot enter mitosis. Therefore this cell death can be rescued by small amount of *Cdc13OP*. Both *Cdc25Δ* and *Slp1Δ* cells can manage endoreplication cycles (brown background) with high amount of Rum1. Endoreplication cells are dead, because they never enter mitosis, but have continuous DNA replication. Deleted mutant of the essential mitotic kinase *cdc13Δ* also show endoreplication cycles in any mutant combination, only the upper limit of the endoreplication is changing.

Yellow background in the table means that the deletion mutants have similar phenotype than wild type cells. If the upper limit is exactly the same as the upper limit in WT cells, then the number is not written in the cell. If the upper limit is lower in the mutant than in wild type, then the number is written with red letters, in other case, when the upper limit is higher in the mutant cell, it is documented in green. Bold coloured letters mean

that there is a huge difference in the upper limit in wild type and in double mutant cells (see figure legend). In this 2 dimensional gTOW analysis it has been clearly shown, that in most cases the robustness of the system is reduced in the double mutant cells. The system, however, is completely unaffected by deletion of some regulatory proteins, such as Cig1 (Bueno and Russell, 1993), Puc1 (Forsburg and Nurse, 1994) and Clp1 (Trautmann et al., 2001). The most important regulatory proteins are Cig2 (Bueno and Russell, 1993), Mik1 (Lundgren et al., 1991), Pyp3 (Millar et al., 1992), Rum1 (Moreno and Nurse, 1994) and Srw1 (Kitamura et al., 1998) in this group. The individual upper limits of these proteins are relatively high (except Rum1), but the deletion of these proteins makes the system more sensitive for the overexpression of other proteins. The robustness is especially decreased when one of the main regulatory Cdk/cyclin complexes, Cdc2/Cig2 is missing. In that case Cdc13 is the only cyclin who can counteract Cdc18, so *cig2Δ* is viable, but only a small amount of extra Cdc18/Cdc10/Mik1 is able to block the cell cycle. The *cig2Δ* cell is also sensitive for Rum1, Srw1 and Slp1, however Cdc25 and Pyp3 levels can be increased highly without any negative effect. Interestingly, the system is in fact sensitive for Pyp3 deletion and reduces the upper limit of many regulatory proteins.

Wee1 deleted cells are small (green background) (Nurse and Thuriaux, 1980), see Cdc13 total level in Table S10. The upper limit of the overexpression was also calculated in these special cases; however the behavior is completely different, the upper limits are therefore also changing differently. Overexpression of most genes causes more serious problems than for wild type cells, but gTOW overexpressions that induce a constant induction of DNA damage response (*Cdc10^{op}*, *Cdc18^{op}*, *Mik1^{op}* on Figure S11C) cause a less serious effect in *wee1* deleted cells. In these cases the damage checkpoint cannot be stabilized without Wee1, which allows the cells to finish cell cycles properly. Of course, the Clp1 overexpression has no effect on Wee1 deletion. These might be some interesting predictions of the model.

10. The “Cdc2-level model”

The extension of the gTOW model with Cdc2 and Cdc2/cyclin complex formation (green on Figure S8) is studied in this chapter.

When the possible competition of cyclins (Cdc13, Cig1, Cig2 and Puc1) for Cdc2 kinase is investigated, the Cdc2 kinase level cannot be neglected anymore. Until this point, high Cdc2 level was assumed, which does not have any rate-limiting role in the activation of Cdk/cyclin complex. Now, the Cdc2 total level is a constant but its complex formation with the cyclins has a significant role in the model. According to the published scientific results (Hayles and Nurse, 1995 and personal communication with J. Hayles) it seems realistic that there are free cyclins present in cells and not all the all of them are bound to Cdc2.

Taking into consideration Cdc2 kinase level, the previous model is extended with Cdc2 and the complex formation of the Cdk/cyclin complexes. Now, all cyclins have a free ($\text{Cycfree} = \text{Cdc13free} + \text{Cig2free} + \text{Cig1free} + \text{Puc1free}$) and a Cdc2 bounded form (lets call them c2c13 , c2ci2 , c2ci1 , and c2pu1 respectively). Each cyclin has an equation with synthesis and degradation parts, except Puc1 that is constant (same as before). The total Cdc2 level is also constant (called Cdc2t). The equations of Cdc13T , Cig1 and Cig2T are the same as before. But now only the Cdc2/cyclin complexes have activity in the cell, and only the Cdc2/Cdc13 and Cdc2/Cig2 complexes can be phosphorylated/dephosphorylated or inhibited by Rum1. Neither Cdc13free nor Cig2free can be regulated by Tyr-phosphorylation or Rum1. So the nomenclature is thus the following:

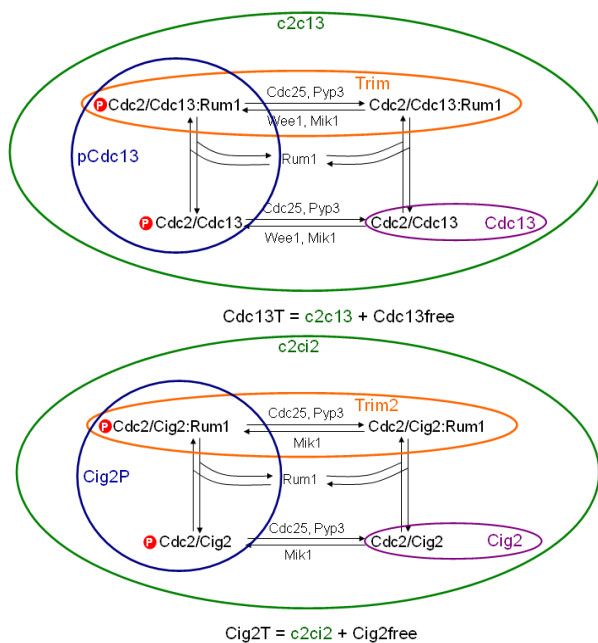


Figure S13. Modeling Cdc2 binding to various cyclins.

As the Cdk/cyclin complex formation is not well-known, it was assumed that all cyclins can bind to Cdc2 with same association and dissociation rates. These reactions are supposed to be fast, the steady state concentration of the dimers (Dim) can thus be calculated in terms of the total pool of cyclin and Cdc2 (Cdc2t).

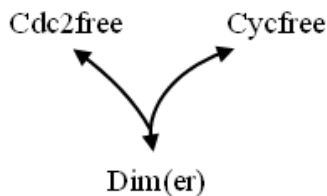
The total cyclin level in the cell:

$$\text{CycT} = \text{Cdc13T} + \text{Cig1} + \text{Cig2T} + \text{Puc1}$$

The total dimer concentration in the cell:

$$\text{Dim} = \text{c2c13} + \text{c2ci1} + \text{c2ci2} + \text{c2pu1}$$

The mechanism of the complex formation and the calculation of the dissociation constant Kdiss) and dimer concentrations are the following:



$$K_{\text{diss}} = \frac{\text{Cdc2free} * \text{Cycfree}}{\text{Dim}} = \frac{(\text{Cdc2T} - \text{Dim}) * (\text{CycT} - \text{Dim})}{\text{Dim}}$$

$$0 = \text{Dim}^2 - \underbrace{(\text{CycT} + \text{Cdc2T} + K_{\text{diss}}) * \text{Dim}}_{\text{BC}} - \text{Cdc2T} * \text{CycT}$$

$$\text{Dim} = \frac{2 * \text{Cdc2T} * \text{CycT}}{\text{BC} + \sqrt{\text{BC}^2 - 4 * \text{Cdc2T} * \text{CycT}}}$$

The concentration of each Cdk/cyclin complex can be calculated using the following rates:

$$\frac{\text{c2c13}}{\text{Dim}} = \frac{\text{Cdc13T}}{\text{CycT}} \quad \frac{\text{c2ci1}}{\text{Dim}} = \frac{\text{Cig1}}{\text{CycT}}$$

$$\frac{\text{c2ci2}}{\text{Dim}} = \frac{\text{Cig2T}}{\text{CycT}} \quad \frac{\text{c2pu1}}{\text{Dim}} = \frac{\text{Puc1}}{\text{CycT}}$$

Then these active forms were replaced everywhere, where the cyclins had effects in the previous model.

The previous model (gTOW_model.ode) is extended with new equations mentioned above (everywhere when Cig1 and Puc1 have effect now c2ci1 and c2p1 are used):

$$\text{CycT} = \text{Cdc13T} + \text{Cig1} + \text{Cig2T} + \text{Puc1}$$

$$\text{BC} = \text{CycT} + \text{Cdc2T} + K_{\text{diss}}$$

$$\text{Dim} = \frac{2 * \text{CycT} * \text{Cdc2T}}{\text{BC} + \sqrt{\text{BC}^2 - 4 * \text{CycT} * \text{Cdc2T}}} - 4 * \text{CycT} * \text{Cdc2T})$$

c2c13 = Dim*Cdc13T/CycT
c2ci1 = Dim*Cig1/CycT
c2ci2 = Dim*Cig2T/CycT
c2pu1 = Dim*Puc1/CycT

Table S12. Testing cyclin competition for Cdc2 *in silico*.

		Kdiss			
		0.01	0.1	1	10
cdc13+	1.5	0.00	0.00	-0.26	
	2	0.00	-0.03	-0.27	
	2.5	0.00	-0.05	-0.28	-0.64
	3	0.00	-0.03	-0.19	-0.63
	3.5	0.00	-0.03	-0.21	-0.63
	4	0.00	-0.03	-0.17	-0.66
	5	0.00	-0.03	-0.20	-0.61
	7.5	0.00	-0.03	-0.10	-0.54
	10	0.00	-0.03	-0.09	-0.47
cig2T	1.5	3.57	3.00	1.14	
	2	0.88	0.88	0.17	
	2.5	0.14	0.23	0.14	-0.98
	3	-0.11	-0.11	-0.06	-0.90
	3.5	0.00	-0.11	-0.19	-0.85
	4	0.00	-0.11	-0.15	-0.79
	5	0.00	-0.11	-0.15	-0.72
	7.5	0.00	-0.11	-0.11	-0.52
	10	0.00	-0.11	-0.06	-0.43
cig1T	1.5	0.25	0.57	6.09	
	2	0.00	0.00	-0.33	
	2.5	0.00	0.00	-0.33	-0.33
	3	0.00	0.00	-0.14	-0.46
	3.5	0.00	0.00	-0.23	-0.52
	4	0.00	0.00	-0.23	-0.57
	5	0.00	0.00	-0.08	-0.53
	7.5	0.00	0.00	-0.09	-0.38
	10	0.00	0.00	0.00	-0.35
puc1T	1.5	5.88	7.57	6.09	
	2	1.70	1.95	1.83	
	2.5	0.59	0.80	1.29	0.80
	3	0.17	0.29	0.94	0.33
	3.5	-0.04	0.00	0.29	0.09
	4	0.00	-0.10	0.07	-0.02
	5	0.00	-0.04	-0.15	-0.25
	7.5	0.00	0.00	-0.09	-0.47
	10	0.00	0.00	-0.07	-0.43

$$\text{delta} = \frac{\text{upper limit of cyclin in } 10X^{\text{cdc2}} - \text{upper limit of cyclin in wild type}}{\text{upper limit of cyclin in wild type}}$$

delta > 0
delta = 0
delta < 0
not calculated

For testing cyclins' competition for Cdc2 *in silico* we analyzed how the upper limit of overexpression of the four cyclins is changing at different Cdc2 total levels (Cdc2t) and Kdiss values (the same dissociation constant of Cdc2/cyclin complex formation is used for all cyclins). The steps of the analysis were the following:

- Kdiss and Cdc2t were changed systematically as indicated to get the same length for the cell cycle the synthesis rate of Cdc13 (k_{sc13}) had to be adjusted in each combination, therefore the WT cycle period remained always 90 min,
- the upper limit of overexpression for all four cyclins is checked at each Cdc2t-Kdiss combination in wild type (WT^{cdc2}) and in 10 times overexpression from the given basal value of cdc2 10X^{cdc2} cells,
- delta = $(10X^{\text{cdc2}} - \text{WT}^{\text{cdc2}}) / \text{WT}^{\text{cdc2}}$ is calculated and detailed in the table at each Cdc2t-Kdiss combination,
- the background of the cell is light yellow if delta is positive, orange if it is negative and dark yellow if it is equal zero (the black cell means that the data could not be calculated. The 90 minutes long cell cycle could not be managed if Kdiss was large and the Cdc2t was small).

Positive number in the table means that 10X^{cdc2} is larger than WT^{cdc2} (light yellow background), the simulations, namely, show that Cdc2 overexpression increases the upper limit of the cyclin overexpression. This behavior can be explained by competition between the cyclins. Positive delta can be managed when both Cdc2 total level and

K_{diss} value are relatively small. Since K_{diss} is small the association between the components is fast, all cyclins are in dimer. Therefore the low Cdc2 level was rate limiting in these reactions, the overexpressed cyclin can extrude the other cyclins from their dimers. When $10X^{cdc2}$ is smaller than WT^{cdc2} , the upper limit of overexpression is higher in WT cells (orange background), which can be implemented with high Cdc2t level and large K_{diss} value. Therefore negative delta means that more Cdc2/cyclin complex can be formed at higher Cdc2 level. In that case the cyclin level is the rate-limiting factor: the binding between Cdc2 and the four different cyclins is weaker; and many unbound cyclins present already at normal Cdc2 concentrations in the cell. When Cdc2t is increasing during overexpression more cyclin can be in complex and more Cdk/cyclin is getting active in the cell, and competition between the cyclins are not taking place. The toxicity is arising from the overexpressed cyclin itself. When $10X^{cdc2} = WT^{cdc2}$, the Cdc2 overexpression has no effect on the cyclin upper limit dark yellow background). It could happen, when the K_{diss} is smaller but Cdc2t is high: the Cdc2 level in WT is high enough to abolish the competition between the cyclins, 10 times more Cdc2 can thus not cause any difference.

The tendency can be seen nicely in these tables. The results correlate with the upper limits of the cyclins' overexpression in WT. The upper limit of Cdc13 is low in WT, so it reaches alone its toxic effect in the cell cycle in all Cdc2t- K_{diss} combinations before the competition between the cyclins would be taken place. However the upper limit of Puc1 is high; therefore in the most cases its negative effect is enforced via competition.

The experimental results have shown that the upper limits of all cyclins are decreasing when Cdc2 is overexpressed in the cell. This means there is no competition between the cyclins. Simulating this realistic situation, a relatively large value should be chosen for the K_{diss} and Cdc2t. This would also predict that in all cases there are Cdc2 free cyclins present in cells.

The `Cdc2_model.ode` file was used for this analysis.

11. References for Supplementary model description and simulation results

- Ayte, J., Schweitzer, C., Zarzov, P., Nurse, P., and DeCaprio, J. A. (2001). Feedback regulation of the MBF transcription factor by cyclin Cig2. *Nature Cell Biol* 3, 1043-1050.
- Basi, G., and Draetta, G. (1995). p13suc1 of *Schizosaccharomyces pombe* regulates two distinct forms of the mitotic cdc2 kinase. *Mol Cell Biol* 15, 2028-2036.
- Baum, B., Wuarin, J., and Nurse, P. (1997). Control of S-phase periodic transcription in the fission yeast mitotic cycle. *Embo J* 16, 4676-4688.
- Benito, J., Martin-Castellanos, C., and Moreno, S. (1998). Regulation of the G1 phase of the cell cycle by periodic stabilization and degradation of the p25rum1 CDK inhibitor. *EMBO J* 17, 482-497.
- Bentley, N. J., Holtzman, D. A., Flaggs, G., Keegan, K. S., DeMaggio, A., Ford, J. C., Hoekstra, M., and Carr, A. M. (1996). The *Schizosaccharomyces pombe* rad3 checkpoint gene. *Embo J* 15, 6641-6651.
- Brown, G. W., Jallepalli, P. V., Huneycutt, B. J., and Kelly, T. J. (1997). Interaction of the S phase regulator cdc18 with cyclin-dependent kinase in fission yeast. *Proc Natl Acad Sci U S A* 94, 6142-6147.
- Bueno, A., and Russell, P. (1993). Two fission yeast B-type cyclins, cig2 and Cdc13, have different functions in mitosis. *Mol Cell Biol* 13, 2286-2297.
- Carr, A. M. (1995). DNA structure checkpoints in fission yeast. *Semin Cell Biol* 6, 65-72.
- Correa-Bordes, J., and Nurse, P. (1995). p25^{rum1} orders S-phase and mitosis by acting as an inhibitor of the p34^{cdc2} mitotic kinase. *Cell* 83, 1001-1009.
- Enoch, T., Carr, A. M., and Nurse, P. (1992). Fission yeast genes involved in coupling mitosis to completion of DNA replication. *Genes Dev* 6, 2035-2046.
- Fisher, D. L., and Nurse, P. (1996). A single fission yeast mitotic cyclin B p34^{cdc2} kinase promotes both S-phase and mitosis in the absence of G1 cyclins. *EMBO J* 15, 850-860.
- Forsburg, S. L., and Nurse, P. (1994). Analysis of the *Schizosaccharomyces pombe* cyclin puc1: evidence for a role in cell cycle exit. *J Cell Sci* 107 (Pt 3), 601-613.
- Grallert, A., Grallert, B., Ribar, B., and Sipiczki, M. (1998). Coordination of initiation of nuclear division and initiation of cell division in *Schizosaccharomyces pombe*: genetic interactions of mutations. *J Bacteriol* 180, 892-900.
- Hayles, J., Fisher, D., Woppard, A., and Nurse, P. (1994). Temporal order of S phase and mitosis in fission yeast is determined by the state of the p34^{cdc2}-mitotic B cyclin complex. *Cell* 78, 813-822.
- Hayles, J., and Nurse, P. (1995). A pre-start checkpoint preventing mitosis in fission yeast acts independently of p34cdc2 tyrosine phosphorylation. *Embo J* 14, 2760-2771.
- Hermand, D., and Nurse, P. (2007). Cdc18 enforces long-term maintenance of the S phase checkpoint by anchoring the Rad3-Rad26 complex to chromatin. *Mol Cell* 26, 553-563.
- Humphrey, T. (2000). DNA damage and cell cycle control in *Schizosaccharomyces*

- pombe. *Mutat Res* 451, 211-226.
- Jallepalli, P. V., Brown, G. W., Muzi-Falconi, M., Tien, D., and Kelly, T. J. (1997). Regulation of the replication initiator protein p65cdc18 by CDK phosphorylation. *Genes Dev* 11, 2767-2779.
- Kelly, T. J., Martin, G. S., Forsburg, S. L., Stephen, R. J., Russo, A., and Nurse, P. (1993). The fission yeast cdc18+ gene product couples S phase to START and mitosis. *Cell* 74, 371-382.
- Kim, S. H., Lin, D. P., Matsumoto, S., Kitazono, A., and Matsumoto, T. (1998). Fission yeast Slp1: an effector of the Mad2-dependent spindle checkpoint. *Science* 279, 1045-1047.
- Kitamura, K., Maekawa, H., and Shimoda, C. (1998). Fission yeast Ste9, a homolog of Hct1/Cdh1 and Fizzy-related, is a novel negative regulator of cell cycle progression during G1-phase. *Mol Biol Cell* 9, 1065-1080.
- Kominami, K., Seth-Smith, H., and Toda, T. (1998). Apc10 and Ste9/Srw1, two regulators of the APC-cyclosome, as well as the CDK inhibitor Rum1 are required for G1 cell-cycle arrest in fission yeast. *Embo J* 17, 5388-5399.
- Kominami, K., and Toda, T. (1997). Fission yeast WD-repeat protein pop1 regulates genome ploidy through ubiquitin-proteasome-mediated degradation of the CDK inhibitor Rum1 and the S-phase initiator Cdc18. *Genes Dev* 11, 1548-1560.
- Labib, K., and Moreno, S. (1996). Rum1: a CDK inhibitor regulating G1 progression in fission yeast. *Trends Cell Biol* 6, 62-66.
- Lopez-Girona, A., Mondesert, O., Leatherwood, J., and Russell, P. (1998). Negative regulation of Cdc18 DNA replication protein by Cdc2. *Mol Biol Cell* 9, 63-73.
- Lundgren, K., Walworth, N., Booher, R., Dembski, M., Kirschner, M., and Beach, D. (1991). mik1 and wee1 cooperate in the inhibitory tyrosine phosphorylation of cdc2. *Cell* 64, 1111-1122.
- Martin-Castellanos, C., Blanco, M. A., de Prada, J. M., and Moreno, S. (2000). The puc1 cyclin regulates the G1 phase of the fission yeast cell cycle in response to cell size. *Mol Biol Cell* 11, 543-554.
- Martin-Castellanos, C., Labib, K., and Moreno, S. (1996). B-type cyclins regulate G1 progression in fission yeast in opposition to the p25rum1 cdk inhibitor. *Embo J* 15, 839-849.
- Martinho, R. G., Lindsay, H. D., Flaggs, G., DeMaggio, A. J., Hoekstra, M. F., Carr, A. M., and Bentley, N. J. (1998). Analysis of Rad3 and Chk1 protein kinases defines different checkpoint responses. *Embo J* 17, 7239-7249.
- McInerny, C. J., Kersey, P. J., Creanor, J., and Fantes, P. A. (1995). Positive and negative roles for cdc10 in cell cycle gene expression. *Nucleic Acids Res* 23, 4761-4768.
- Millar, J. B., Lenaers, G., and Russell, P. (1992). Pyp3 PTPase acts as a mitotic inducer in fission yeast. *Embo J* 11, 4933-4941.
- Mondesert, O., McGowan, C. H., and Russell, P. (1996). Cig2, a B-type cyclin, promotes the onset of S in *Schizosaccharomyces pombe*. *Mol Cell Biol* 16, 1527-1533.
- Moreno, S., and Nurse, P. (1994). Regulation of progression through the G1 phase of the cell cycle by the rum1+ gene. *Nature* 367, 236-242.

- Morgan, D. O. (1999). Regulation of the APC and the exit from mitosis. *Nature Cell Biol* 1, E47-E53.
- Ng, S. S., Anderson, M., White, S., and McInerny, C. J. (2001). mik1(+) G1-S transcription regulates mitotic entry in fission yeast. *FEBS Lett* 503, 131-134.
- Nishitani, H., and Nurse, P. (1995). p65cdc18 plays a major role controlling the initiation of DNA replication in fission yeast. *Cell* 83, 397-405.
- Novak, B., Pataki, Z., Ciliberto, A., and Tyson, J. J. (2001). Mathematical model of the cell division cycle of fission yeast. *Chaos* 1, 277-286.
- Nurse, P. (1990). Universal control mechanism regulating onset of M-phase. *Nature* 344, 503-508.
- Nurse, P. (1999). Cyclin dependent kinases and regulation of the fission yeast cell cycle. *Biol Chem* 380, 729-733.
- Nurse, P., and Thuriaux, P. (1980). Regulatory genes controlling mitosis in the fission yeast *Schizosaccharomyces pombe*. *Genetics* 96, 627-637.
- Peters, J. M. (2002). The anaphase-promoting complex: proteolysis in mitosis and beyond. *Mol Cell* 9, 931-943.
- Rhind, N., and Russell, P. (1998). Tyrosine phosphorylation of cdc2 is required for the replication checkpoint in *Schizosaccharomyces pombe*. *Mol Cell Biol* 18, 3782-3787.
- Russell, P., and Nurse, P. (1986). cdc25⁺ functions as an inducer in the mitotic control of fission yeast. *Cell* 45, 145-153.
- Sveiczer, A., Csikasz-Nagy, A., Gyorffy, B., Tyson, J. J., and Novak, B. (2000). Modeling the fission yeast cell cycle: quantized cycle times in wee1- cdc25Delta mutant cells. *Proc Natl Acad Sci U S A* 97, 7865-7870.
- Sveiczer, A., Novak, B., and Mitchison, J. M. (1996). The size control of fission yeast revisited. *J Cell Sci* 109 (Pt 12), 2947-2957.
- Sveiczer, A., Tyson, J. J., and Novak, B. (2004). Modelling the fission yeast cell cycle. *Brief Funct Genomic Proteomic* 2, 298-307.
- Trautmann, S., Wolfe, B. A., Jorgensen, P., Tyers, M., Gould, K. L., and McCollum, D. (2001). Fission yeast Clp1p phosphatase regulates G2/M transition and coordination of cytokinesis with cell cycle progression. *Current Biology* 11, 931-940.
- Yamaguchi, S., Okayama, H., and Nurse, P. (2000). Fission yeast Fizzy-related protein srw1p is a G(1)-specific promoter of mitotic cyclin B degradation. *EMBO J* 19, 3968-3977.
- Yamano, H., Kominami, K., Harrison, C., Kitamura, K., Katayama, S., Dhut, S., Hunt, T., and Toda, T. (2004). Requirement of the SCFPop1/Pop2 Ubiquitin Ligase for Degradation of the Fission Yeast S Phase Cyclin Cig2. *J Biol Chem* 279, 18974-18980. Epub 2004 Feb 18916.
- Zarzov, P., Decottignies, A., Baldacci, G., and Nurse, P. (2002). G(1)/S CDK is inhibited to restrain mitotic onset when DNA replication is blocked in fission yeast. *Embo J* 21, 3370-3376.